Contents

[1] Our treatment is based on Burke (1970).

Chapter 16

Waves and Convection

Version 1016.1.K, 25 February 2009. *Please send comments, suggestions, and errata via email to kip@caltech.edu or on paper to Kip Thorne, 350-17 Caltech, Pasadena CA 91125*

Box 16.1
Reader's Guide

- This chapter relies heavily on Chaps. 12 and 13.
- Chap. 16 (compressible flows) relies to some extent on Secs. 16.2, 16.3 and 16.5 of this chapter.
- The remaining chapters of this book do not rely significantly on this chapter.

16.1 Overview

In the preceding chapters, we have derived the basic equations of fluid dynamics and developed a variety of techniques to describe stationary flows. We have also demonstrated how, even if there exists a rigorous, stationary solution of these equations for a time-steady flow, instabilities may develop and the amplitude of oscillatory disturbances can grow with time. These unstable modes of an unstable flow can usually be thought of as waves that interact strongly with the flow and extract energy from it. Waves, though, are quite general and can be studied quite independently of their sources. Fluid dynamical waves come in a wide variety of forms. They can be driven by a combination of gravitational, pressure, rotational and surface-tension stresses and also by mechanical disturbances, such as water rushing past a boat or air passing through a larynx. In this chapter, we shall describe a few examples of wave modes in fluids, chosen to illustrate general wave properties.

The most familiar types of wave are probably gravity waves on a large body of water (Sec. 16.2), e.g. ocean waves and waves on the surfaces of lakes and rivers. We consider these in the linear approximation and find that they are dispersive in general, though they become

nondispersive in the long-wavelength (shallow-water) limit. We shall illustrate gravity waves by their roles in *helioseismology*, the study of coherent-wave modes excited within the body of the sun by convective overturning motions. We shall also examine the effects of surface tension on gravity waves, and in this connection shall develop a mathematical description of surface tension (Box 16.2).

In contrast to the elastodynamic waves of Chap. 11, waves in fluids often develop amplitudes large enough that nonlinear effects become important (Sec. 16.3). The nonlinearities can cause the front of a wave to steepen and then break—a phenomenon we have all seen at the sea shore. It turns out that, at least under some restrictive conditions, nonlinear waves have some very surprising properties. There exist *soliton* or *solitary-wave* modes in which the front-steepening due to nonlinearity is stably held in check by dispersion, and particular wave profiles are quite robust and can propagate for long intervals of time without breaking or dispersing. We shall demonstrate this by studying flow in a shallow channel. We shall also explore the remarkable behaviors of such solitons when they pass through each other.

In a nearly rigidly rotating fluid, there is a remarkable type of wave in which the restoring force is the Coriolis effect, and which have the unusual property that their group and phase velocities are oppositely directed. These so-called Rossby waves, studied in Sec. 16.4, are important in both the oceans and the atmosphere.

The simplest fluid waves of all are small-amplitude sound waves—a paradigm for scalar waves. These are nondispersive, just like electromagnetic waves, and are therefore sometimes useful for human communication. We shall study sound waves in Sec.16.5 and shall use them to explore an issue in fundamental physics: the radiation reaction force that acts back on a wave-emitting object. We shall also explore how sound waves can be produced by fluid flows. This will be illustrated with the problem of sound generation by high-speed turbulent flows—a problem that provides a good starting point for the topic of the following chapter, compressible flows.

The last section of this chapter, Sec. 16.6, deals with dynamical motions of a fluid that are driven by thermal effects, *convection*. To understand convection, one must first understand diffusive head conduction.

When viewed microscopically, heat conduction is a similar transport process to viscosity, and it is responsible for analogous physical effects. If a viscous fluid has high viscosity, then vorticity diffuses through it rapidly; simularly, if a fluid has high thermal conductivity, then heat diffuses through it rapidly. In the other extreme, when viscosity is low (i.e., when the Reynolds number is high), instabilities produce turbulence, which transports vorticity far more rapidly than diffusion could possibly do. Analogously, in heated fluids with modest conductivity, the accumulation of heat drives the fluid into convective motion and the heat is transported much more efficiently by this motion than by thermal conduction alone. As the convective heat transport increases, the fluid motion becomes more vigorous and, if the viscosity is sufficiently low, the thermally driven flow can also become turbulent. These effects are very much in evidence near solid boundaries, where thermal boundary layers can be formed, analogous to viscous boundary layers.

In addition to thermal effects that resemble the effects of viscosity, there are also unique thermal effects—particularly the novel and subtle combined effects of gravity and heat. Heat,

unlike vorticity, causes a fluid to expand and thus, in the presence of gravity, to become buoyant; and this buoyancy can drive thermal circulation or *free convection* in an otherwise stationary fluid. (Free convection should be distinguished from *forced convection* in which heat is carried passively by a flow driven in the usual manner by externally imposed pressure gradients, for example when you blow on hot food to cool it.)

The transport of heat is a fundamental characteristic of many flows. It dictates the form of global weather patterns and ocean currents. It is also of great technological importance and is studied in detail, for example, in the cooling of nuclear reactors and the design of automobile engines. From a more fundamental perspective, as we have already discussed, the analysis and experimental studies of convection have led to major insights into the route to chaos (cf. Sec. 14.5).

In Sec. 16.6, we shall describe some flows where thermal effects are predominant. We shall begin in Sec. 16.6.1 by modifying the conservation laws of fluid dynamics so as to incorporate heat conduction. Then in Sec. 16.6.2 we shall discuss the *Boussinesq approximation*, which is appropriate for modest scale flows where buoyancy is important. This allows us in Sec. 16.6.3 to derive the conditions under which convection is initiated. Unfortunately, this Boussinesq approximation sometimes breaks down. In particular, as we discuss in Sec. 16.6.4, it is inappropriate for application to convection in stars and planets where circulation takes place over several gravitational scale heights. Here, we shall have to use alternative, more heuristic arguments to derive the relevant criterion for convective instability, known as the *Schwarzschild criterion*, and to quantify the associated heat flux. We shall apply this theory to the solar convection zone.

Finally, in Sec. 16.6.5 we return to simple buoyancy-driven convection in a stratified fluid to consider *double diffusion*, a quite general type of instability which can arise when the diffusion of two physical quantities (in our case heat and the concentration of salt) render a fluid unstable despite the fact that the fluid would be stably stratified if there were only concentration gradients of one of these quantities.

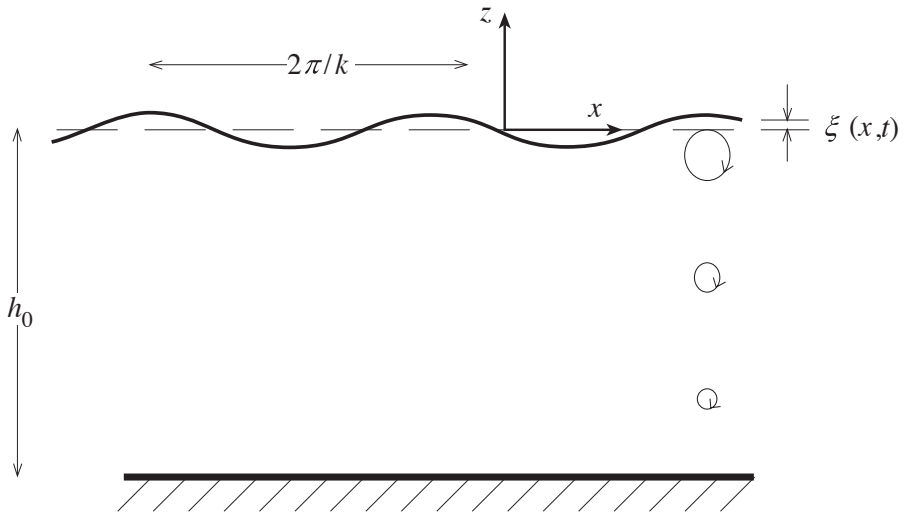

Fig. 16.1: Gravity Waves propagating horizontally across a lake of depth h_o.

16.2 Gravity Waves on the Surface of a Fluid

Gravity waves[1] are waves on and beneath the surface of a fluid, for which the restoring force is the downward pull of gravity. Familiar examples are ocean waves and the waves produced on the surface of a pond when a pebble is thrown in. Less familiar are "g-modes" of vibration of the sun, discussed at the end of this section.

Consider a small-amplitude wave propagating along the surface of a flat-bottomed lake with depth h_o, as shown in Fig. 16.1. As the water's displacement is small, we can describe the wave as a linear perturbation about equilibrium. The equilibrium water is at rest, i.e. it has velocity $\mathbf{v} = 0$. The water's perturbed motion is essentially inviscid and incompressible, so $\boldsymbol{\nabla} \cdot \mathbf{v} = 0$. A simple application of the equation of vorticity transport, Eq. (13.3), assures us that since the water is static and thus irrotational before and after the wave passes, it must also be irrotational within the wave. Therefore, we can describe the wave inside the water by a velocity potential ψ whose gradient is the velocity field,

$$\mathbf{v} = \boldsymbol{\nabla}\psi \ . \tag{16.1}$$

Incompressibility, $\boldsymbol{\nabla} \cdot \mathbf{v} = 0$, applied to this equation, implies that the velocity potential ψ satisfies Laplace's equation

$$\nabla^2\psi = 0 \tag{16.2}$$

We introduce horizontal coordinates x, y and a vertical coordinate z measured upward from the lake's equilibrium surface (cf. Fig. 16.1), and for simplicity we confine attention to a sinusoidal wave propagating in the x direction with angular frequency ω and wave number k. Then ψ and all other perturbed quantities will have the form $f(z)\exp[i(kx-\omega t)]$ for some function $f(z)$. More general disturbances can be expressed as a superposition of many of these elementary wave modes propagating in various horizontal directions (and in the limit, as a Fourier integral). All of the properties of such superpositions follow straightforwardly from those of our elementary plane-wave mode, so we shall continue to focus on it.

We must use Laplace'e equation (16.2) to solve for the vertical variation, $f(z)$, of the velocity potential. As the horizontal variation at a particular time is $\propto \exp(ikx)$, direct substitution into Eq. (16.2) gives two possible vertical variations, $\psi \propto \exp(\pm kz)$. The precise linear combination of these two forms is dictated by the boundary conditions. The one that we shall need is that the vertical component of velocity $v_z = \partial\psi/\partial z$ vanish at the bottom of the lake ($z = -h_o$). The only combination that can vanish is a sinh function. Its integral, the velocity potential, therefore involves a cosh function:

$$\psi = \psi_0 \cosh[k(z + h_o)]\ \exp[i(kx - \omega t)]. \tag{16.3}$$

An alert reader might note at this point that the *horizontal* velocity does not vanish at the lake bottom, whereas a no-slip condition should apply in practice. In fact, as we discussed in Sec 13.4, a thin, viscous boundary layer along the bottom of the lake will join our potential-flow solution (16.3) to nonslipping fluid at the bottom. We shall ignore the

[1]Not to be confused with *gravitational waves* which are waves in the gravitational field that propagate at the speed of light and which we shall meet in Chap. 25

boundary layer under the (justifiable) assumption that for our oscillating waves it is too thin to affect much of the flow.

Returning to the potential flow, we must also impose a boundary condition at the surface. This can be obtained from Bernoulli's law. The version of Bernoulli's law that we need is that for an irrotational, isentropic, time-varying flow:

$$\mathbf{v}^2/2 + h + \Phi + \partial\psi/\partial t = \text{constant everywhere in the flow} \tag{16.4}$$

[Eqs. (12.46), (12.50)]. We shall apply this law at the surface of the perturbed water. Let us examine each term: (i) The term $\mathbf{v}^2/2$ is quadratic in a perturbed quantity and therefore can be dropped. (ii) The enthalpy $h = u + P/\rho$ (cf. Box 12.1) is a constant since u and ρ are constants throughout the fluid and P is constant on the surface and equal to the atmospheric pressure. [Actually, there will be a slight variation of the surface pressure caused by the varying weight of the air above the surface, but as the density of air is typically $\sim 10^{-3}$ that of water, this is a very small correction.] (iii) The gravitational potential at the fluid surface is $\Phi = g\xi$, where $\xi(x,t)$ is the surface's vertical displacement from equilibrium and we ignore an additive constant. (iv) The constant on the right hand side, which could depend on time $C(t)$, can be absorbed into the velocity potential term $\partial\psi/\partial t$ without changing the physical observable $\mathbf{v} = \boldsymbol{\nabla}\psi$. Bernoulli's law applied at the surface therefore simplifies to give

$$g\xi + \frac{\partial\psi}{\partial t} = 0\ . \tag{16.5}$$

Now, the vertical component of the surface velocity in the linear approximation is just $v_z(z=0,t) = \partial\xi/\partial t$. Expressing v_z in terms of the velocity potential we then obtain

$$\frac{\partial\xi}{\partial t} = v_z = \frac{\partial\psi}{\partial z}\ . \tag{16.6}$$

Combining this with the time derivative of Eq. (16.5), we obtain an equation for the vertical gradient of ψ in terms of its time derivative:

$$g\frac{\partial\psi}{\partial z} = -\frac{\partial^2\psi}{\partial t^2}. \tag{16.7}$$

Finally, substituting Eq. (16.3) into Eq. (16.7) and setting $z = 0$ [because we derived Eq. (16.7) only at the water's surface], we obtain the dispersion relation for linearized gravity waves:

$$\boxed{\omega^2 = gk\tanh(kh_o)} \tag{16.8}$$

How do the individual elements of fluid move in a gravity wave? We can answer this question by first computing the vertical and horizontal components of the velocity by differentiating Eq. (16.3) [Ex. 16.1]. We find that the fluid elements undergo elliptical motion similar to that found for Rayleigh waves on the surface of a solid (Sec.11.4). However, in gravity waves, the sense of rotation of the particles is always the same at a particular phase of the wave, in contrast to reversals found in Rayleigh waves.

We now consider two limiting cases: deep water and shallow water.

16.2.1 Deep Water Waves

When the water is deep compared to the wavelength of the waves, $kh_o \gg 1$, the dispersion relation (16.8) is approximately

$$\boxed{\omega = \sqrt{gk}\ .} \tag{16.9}$$

Thus, deep water waves are dispersive; their group velocity $V_g \equiv d\omega/dk = \frac{1}{2}\sqrt{g/k}$ is half their phase velocity, $V_\phi \equiv \omega/k = \sqrt{g/k}$. [Note: We could have deduced the deep-water dispersion relation (16.9), up to a dimensionless multiplicative constant, by dimensional arguments: The only frequency that can be constructed from the relevant variables g, k, ρ is $\sqrt{gk}$.]

16.2.2 Shallow Water Waves

For shallow water waves, with $kh_o \ll 1$, the dispersion relation (16.8) becomes

$$\boxed{\omega = \sqrt{gh_o}\,k\ .} \tag{16.10}$$

Thus, these waves are nondispersive; their phase and group velocities are $V_\phi = V_g = \sqrt{gh_o}$.

Below, when studying solitons, we shall need two special properties of shallow water waves. First, when the depth of the water is small compared with the wavelength, but not very small, the waves will be slightly dispersive. We can obtain a correction to Eq. (16.10) by expanding the tanh function of Eq. (16.8) as $\tanh x = x - x^3/3 + \ldots$. The dispersion relation then becomes

$$\omega = \sqrt{gh_o}\left(1 - \frac{1}{6}k^2h_o^2\right)k\ . \tag{16.11}$$

Second, by computing $\mathbf{v} = \boldsymbol{\nabla}\psi$ from Eq. (16.3), we find that *in the shallow-water limit the horizontal motions are much larger than the vertical motions, and are essentially independent of depth.* The reason, physically, is that the fluid acceleration is produced almost entirely by a horizontal pressure gradient (caused by spatially variable water depth) that is independent of height; see Ex. 16.1.

16.2.3 Capillary Waves

When the wavelength is very short (so k is very large), we must include the effects of *surface tension* on the surface boundary condition. This can be done by a very simple, heuristic argument. Surface tension is usually treated as an isotropic force per unit length, γ, that lies in the surface and is unaffected by changes in the shape or size of the surface; see Box 16.2. In the case of a gravity wave, this tension produces on the fluid's surface a net downward force per unit area $-\gamma d^2\xi/dx^2 = \gamma k^2\xi$, where k is the horizontal wave number. [This downward force is like that on a curved violin string; cf. Eq. (11.27) and associated discussion.] This additional force must be included in Eq. (16.5) as an augmentation of ρg. Correspondingly, the effect of surface tension on a mode with wave number k is simply to change the true

Box 16.2
Surface Tension

In a water molecule, the two hydrogen atoms stick out from the larger oxygen atom somewhat like Micky Mouse's ears, with an H-O-H angle of 105 degrees. This asymmetry of the molecule gives rise to a rather large electric dipole moment. In the interior of a body of water, the dipole moments are oriented rather randomly, but near the water's surface they tend to be parallel to the surface and bond with each other so as to create *surface tension* — a macroscopically isotropic, two-dimensional tension force (force per unit length) γ that is confined to the water's surface.

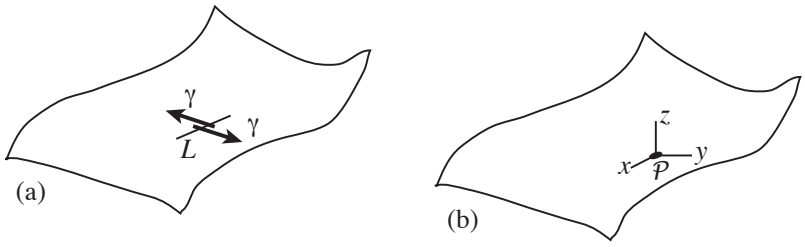

More specifically, consider a line L in the water's surface, with unit length [drawing (a) above]. The surface water on one side of L exerts a tension (pulling) force on the surface water on the other side. The magnitude of this force is γ and it is orthogonal to the line L regardless of L's orientation. This is analogous to an isotropic pressure P in three dimensions, which acts orthogonally across any unit area.

Choose a point $\mathcal{P}$ in the water's surface and introduce local Cartesian coordinates there with x and y lying in the surface and z orthogonal to it [drawing (b) above]. In this coordinate system, the 2-dimensional stress tensor associated with surface tension has components ${}^{(2)}T_{xx} = {}^{(2)}T_{yy} = -\gamma$, analogous to the 3-dimensional stress tensor for an isotropic pressure, $T_{xx} = T_{yy} = T_{zz} = P$. We can also use a 3-dimensional stress tensor to describe the surface tension: $T_{xx} = T_{yy} = -\gamma\delta(z)$; all other $T_{jk} = 0$. If we integrate this 3-dimensional stress tensor through the water's surface, we obtain the 2-dimensional stress tensor: $\int T_{jk}dz = {}^{(2)}T_{jk}$; i.e., $\int T_{xx}dz = \int T_{yy}dz = -\gamma$. The 2-dimensional metric of the surface is ${}^{(2)}\mathbf{g} = \mathbf{g} - \mathbf{e}_z \otimes \mathbf{e}_z$; in terms of this 2-dimensional metric, the surface tension's 3-dimensional stress tensor is $\mathbf{T} = -\gamma\delta(z){}^{(2)}\mathbf{g}$.

Water is not the only fluid that exhibits surface tension; all fluids do so, at the interfaces between themselves and other substances. For a thin film, e.g. a soap bubble, there are two interfaces (the top face and the bottom face of the film), so the stress tensor is twice as large as for a single surface, $\mathbf{T} = -2\gamma\delta(z){}^{(2)}\mathbf{g}$.

The hotter the fluid, the more randomly are oriented its surface molecules and hence the smaller the fluid's surface tension γ. For water, γ varies from 75.6 dyne/cm^2 at $T = 0$ C, to 72.0 dyne/cm^2 at $T = 25$ C, to 58.9 dyne/cm^2 at $T = 100$ C.

In Exs. 16.3 and 16.4 we explore some applications of surface tension. In Sec. 16.2.3 and Ex. 16.5 we explore the influence of surface tension on water waves.

gravity to an *effective gravity*

$$g \to g + \frac{\gamma k^2}{\rho} \ . \tag{16.12}$$

The remainder of the derivation of the dispersion relation for deep gravity waves carries over unchanged, and the dispersion relation becomes

$$\boxed{\omega^2 = gk + \frac{\gamma k^3}{\rho}} \tag{16.13}$$

[cf. Eqs. (16.9) and (16.12)]. When the second term dominates, the waves are sometimes called *capillary waves*.

16.2.4 Helioseismology

The sun provides an excellent example of the excitation of small amplitude waves in a fluid body. In the 1960s, Robert Leighton and colleagues discovered that the surface of the sun oscillates vertically with a period of roughly five minutes and a speed of ~ 1 km s^{-1}. This was thought to be an incoherent surface phenomenon until it was shown that the observed variation was, in fact, the superposition of thousands of highly coherent wave modes excited within the sun's interior — normal modes of the sun. Present day techniques allow surface velocity amplitudes as small as 2 mm s^{-1} to be measured, and phase coherence for intervals as long as a year has been observed. Studying the frequency spectrum and its variation provides a unique probe of the sun's interior structure, just as the measurement of conventional seismic waves, as described in Sec.11.4, probes the earth's interior.

The description of the normal modes of the sun requires some modification of our treatment of gravity waves. We shall eschew details and just outline the principles. First, the sun is (very nearly) spherical. We therefore work in spherical polar coordinates rather than Cartesian coordinates. Second, the sun is made of hot gas and it is no longer a good approximation to assume that the fluid is always incompressible. We must therefore replace the equation $\nabla \cdot \mathbf{v} = 0$ with the full equation of continuity (mass conservation) together with the equation of energy conservation which governs the relationship between the density and pressure perturbations. Third, the sun is not uniform. The pressure and density in the unperturbed gas vary with radius in a known manner and must be included. Fourth, the sun has a finite surface area. Instead of assuming that there will be a continuous spectrum of waves, we must now anticipate that the boundary conditions will lead to a discrete spectrum of normal modes. Allowing for these complications, it is possible to derive a differential equation to replace Eq. (16.7). It turns out that a convenient dependent variable (replacing the velocity potential ψ) is the pressure perturbation. The boundary conditions are that the displacement vanish at the center of the sun and that the pressure perturbation vanish at the surface.

At this point the problem is reminiscent of the famous solution for the eigenfunctions of the Schrödinger equation for a hydrogen atom in terms of associated Laguerre polynomials. The wave frequencies of the sun's normal modes are given by the eigenvalues of the differential equation. The corresponding eigenfunctions can be classified using three quantum

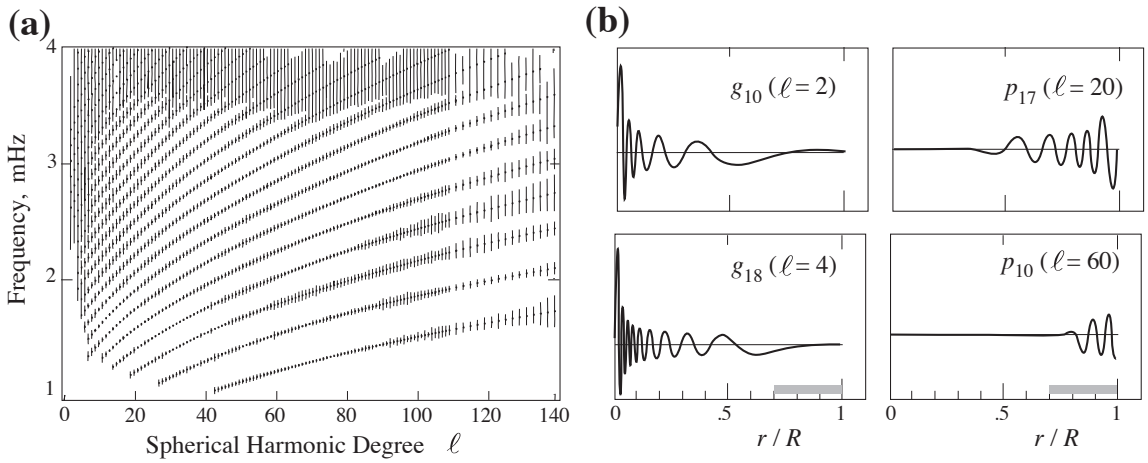

Fig. 16.2: (a) Measured frequency spectrum for solar p-modes with different values of the quantum numbers n, l. The error bars are magnified by a factor 1000. Frequencies for modes with $n > 30$ and $l > 1000$ have been measured. (b) Sample eigenfunctions for g and p modes labeled by n (subscripts) and l (parentheses). The ordinate is the radial velocity and the abscissa is fractional radial distance from the sun's center to its surface. The solar convection zone is the dashed region at the bottom. (Adapted from Libbrecht and Woodard 1991.)

numbers, n, l, m, where n counts the number of radial nodes in the eigenfunction and the angular variation is proportional to the spherical harmonic $Y_l^m(\theta, \phi)$. If the sun were precisely spherical, the modes that are distinguished only by their m quantum number would be degenerate just as is the case with an atom when there is no preferred direction in space. However, the sun rotates with a latitude-dependent period in the range $\sim 25 - 30$ days and this breaks the degeneracy just as an applied magnetic field in an atom breaks the degeneracy of the atom's states (the Zeeman effect). From the splitting of the solar-mode spectrum, it is possible to learn about the distribution of rotational angular momentum inside the sun.

When this problem is solved in detail, it turns out that there are two general classes of modes. One class is similar to gravity waves, in the sense that the forces which drive the gas's motions are produced primarily by gravity (either directly, or indirectly via the weight of overlying material producing pressure that pushes on the gas.) These are called *g modes*. In the second class (known as *p* and *f modes*), the pressure forces arise mainly from the compression of the fluid just like in sound waves (which we shall study in Sec. 16.5 below). Now, it turns out that the g modes have large amplitudes in the middle of the sun, whereas the p and f modes are dominant in the outer layers [cf. Fig. 16.2(b)]. The reasons for this are relatively easy to understand and introduce ideas to which we shall return:

The sun is a hot body, much hotter at its center ($T \sim 1.5 \times 10^7$ K) than on its surface ($T \sim 6000$ K). The sound speed c is therefore much greater in its interior and so p and f modes of a given frequency ω can carry their energy flux $\sim \rho\xi^2\omega^2 c$ (Sec.16.5) with much smaller amplitudes ξ than near the surface. That is why the p- and f-mode amplitudes are much smaller in the center of the sun than near the surface.

The g-modes are controlled by different physics and thus behave differently: The outer ~ 30 percent (by radius) of the sun is *convective* (cf. Sec. 16.6.4) because the diffusion of

photons is inadequate to carry the huge amount of nuclear energy being generated in the solar core. The convection produces an equilibrium variation of pressure and density with radius that are just such as to keep the sun almost neutrally stable, so that regions that are slightly hotter (cooler) than their surroundings will rise (sink) in the solar gravitational field. Therefore there cannot be much of a mechanical restoring force which would cause these regions to oscillate about their average positions, and so the g modes (which are influenced almost solely by gravity) have little restoring force and thus are *evanescent* in the convection zone, and so their amplitudes decay quickly with increasing radius there.

We should therefore expect only p and f modes to be seen in the surface motions and this is, indeed the case. Furthermore, we should not expect the properties of these modes to be very sensitive to the physical conditions in the core. A more detailed analysis bears this out.

****

EXERCISES

Exercise 16.1 *Problem: Fluid Motions in Gravity Waves*

(a) Show that in a gravity wave in water of arbitrary depth, each fluid element undergoes elliptical motion. (Assume that the amplitude of the water's displacement is small compared to a wavelength.)

(b) Calculate the longitudinal diameter of the motion's ellipse, and the ratio of vertical to longitudinal diameters, as functions of depth.

(c) Show that for a deep-water wave, $kh_o \gg 1$, the ellipses are all circles with diameters that die out exponentially with depth.

(d) We normally think of a circular motion of fluid as entailing vorticity, but a gravity wave in water has vanishing vorticity. How can this vanishing vorticity be compatible with the circular motion of fluid elements?

(e) Show that for a shallow-water wave, $kh_o \ll 1$, the motion is (nearly) horizontal and independent of height z.

(f) Compute the pressure perturbation $P(x, z)$ inside the fluid for arbitrary depth. Show that, for a shallow-water wave the pressure is determined by the need to balance the weight of the overlying fluid, but for general depth, vertical fluid accelerations alter this condition of weight balance.

Exercise 16.2 *Problem: Maximum size of a water droplet*
What is the maximum size of water droplets that can form by water very slowly dripping out of a pipette? and out of a water faucet?

Exercise 16.3 *Problem: Force balance for an interface between two fluids*
Consider a point $\mathcal{P}$ in the curved interface between two fluids. Introduce Cartesian coordinates at $\mathcal{P}$ with x and y parallel to the interface and z orthogonal [as in diagram (b) of Box 16.2], and orient the x and y axes along the directions of the interface's "principal curvatures", so the local equation for the interface is

$$z = \frac{x^2}{2R_1} + \frac{y^2}{2R_2} \ . \tag{16.14}$$

Here R_1 and R_2 are the surface's "principal radii of curvature" at $\mathcal{P}$; note that each of them can be positive or negative, depending on whether the surface bends up or down along their directions. Show that stress balance $\boldsymbol{\nabla} \cdot \mathbf{T} = 0$ for the surface implies that the pressure difference across the surface is

$$\boxed{\Delta P = \gamma \left(\frac{1}{R_1} + \frac{1}{R_2} \right) \ ,} \tag{16.15}$$

where γ is the surface tension.

Exercise 16.4 *Challenge: Minimum Area of Soap Film*
For a soap film that is attached to a bent wire (e.g. to the circular wire that a child uses to blow a bubble), the air pressure on the film's two sides is the same. Therefore, Eq. (16.15) (with γ replaced by 2γ since the film has two faces) tells us that at every point of the film, its two principal radii of curvature must be equal and opposite, $R_1 = -R_2$. It is an interesting excercise in differential geometry to show that this means that the soap film's surface area is an extremum with respect to variations of the film's shape, holding its boundary on the wire fixed. If you know enough differential geometry, prove this extremal-area property of soap films, and then show that, in order for the film's shape to be stable, its extremal area must actually be a minimum.

Exercise 16.5 *Problem: Capillary Waves*
Consider deep-water gravity waves of short enough wavelength that surface tension must be included, so the dispersion relation is Eq. (16.13). Show that there is a minimum value of the group velocity and find its value together with the wavelength of the associated wave. Evaluate these for water ($\gamma \sim 0.07$ N m^{-1}). Try performing a crude experiment to verify this phenomenon.

Exercise 16.6 *Example: Boat Waves*
A toy boat moves with uniform velocity $\mathbf{u}$ across a deep pond (Fig. 16.3). Consider the wave pattern (time-independent in the boat's frame) produced on the water's surface at distances large compared to the boat's size. Both gravity waves and surface-tension or *capillary* waves are excited. Show that capillary waves are found both ahead of and behind the boat, and gravity waves, solely inside a trailing wedge. More specifically:

(a) In the rest frame of the water, the waves' dispersion relation is Eq. (16.13). Change notation so ω is the waves' angular velocity as seen in the boat's frame and ω_o in the

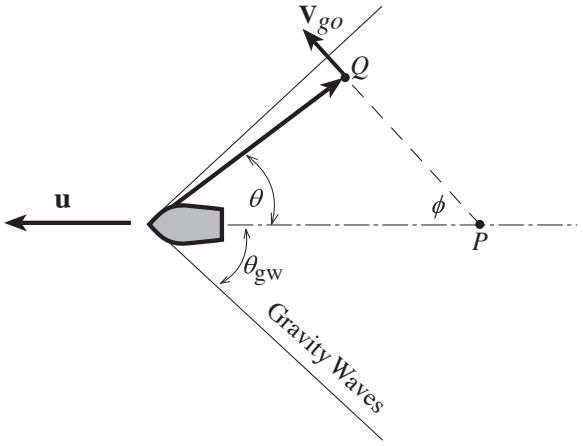

Fig. 16.3: Capillary and Gravity waves excited by a small boat (Ex. 16.6).

water's frame, so the dispersion relation is $\omega_o^2 = gk + (\gamma/\rho)k^3$. Use the doppler shift (i.e. the transformation between frames) to derive the boat-frame dispersion relation $\omega(k)$.

(b) The boat radiates a spectrum of waves in all directions. However, only those with vanishing frequency in the boat's frame, $\omega = 0$, contribute to the time-independent ("stationary") pattern. As seen in the water's frame and analyzed in the geometric optics approximation of Chap. 6, these waves are generated by the boat (at points along its dash-dot trajectory in Fig. 16.3) and travel outward with the group velocity $\mathbf{V}_{go}$. Regard Fig. 16.3 as a snapshot of the boat and water at a particular moment of time. Consider a wave that was generated at an earlier time, when the boat was at location $\mathcal{P}$, and that traveled outward from there with speed V_{go} at an angle ϕ to the boat's direction of motion. (You may restrict yourself to $0 \le \phi \le \pi/2$.) Identify the point $\mathcal{Q}$ that this wave has reached, at the time of the snapshot, by the angle θ shown in the figure. Show that θ is given by

$$\tan\theta = \frac{V_{go}(k)\sin\phi}{u - V_{go}(k)\cos\phi} \ , \tag{16.16a}$$

where k is determined by the dispersion relation $\omega_0(k)$ together with the "vanishing ω" condition

$$\omega_0(k,\phi) = uk\cos\phi \ . \tag{16.16b}$$

(c) Specialize to capillary waves [$k \gg \sqrt{g\rho/\gamma}$]. Show that

$$\tan\theta = \frac{3\tan\phi}{2\tan^2\phi - 1} \ . \tag{16.17}$$

Demonstrate that the capillary wave pattern is present for all values of θ (including in front of the boat, $\pi/2 < \theta < \pi$, and behind it, $0 \le \theta \le \pi/2$).

(d) Next, specialize to gravity waves and show that

$$\tan\theta = \frac{\tan\phi}{2\tan^2\phi + 1} \ . \tag{16.18}$$

Demonstrate that the gravity-wave pattern is confined to a trailing wedge with angles $\theta < \theta_{\rm gw} = \sin^{-1}(1/3) = 19.47^{\rm o}$; cf. Fig. 16.3. You might try to reproduce these results experimentally.

Exercise 16.7 *Example: Shallow-Water Waves with Variable Depth; Tsunamis*[2]
Consider shallow-water waves in which the height of the bottom boundary varies, so the unperturbed water's depth is variable $h_o = h_o(x, y)$.

(a) Show that the wave equation for the perturbation $\xi(x, y, t)$ of the water's height takes the form

$$\frac{\partial^2\xi}{\partial t^2} - \boldsymbol{\nabla}\cdot(gh_o\boldsymbol{\nabla}\xi) = 0 \ . \tag{16.19}$$

Note that gh_o is the square of the wave's propagation speed c^2 (phase speed and group speed), so this equation takes the form that we studied in the geometric optics approximation in Sec. 6.3.1.

(b) Describe what happens to the direction of propagation of a wave as the depth h_o of the water varies (either as a set of discrete jumps in h_o or as a slowly varying h_o). As a specific example, how must the propagation direction change as waves approach a beach (but when they are sufficiently far out from the beach that nonlinearities have not yet caused them to begin to break). Compare with your own observations at a beach.

(c) Tsunamis are waves with enormous wavelengths, ~ 100 km or so, that propagate on the deep ocean. Since the ocean depth is typically ~ 4 km, tsunamis are governed by the shallow-water wave equation (16.19). What would you have to do to the ocean floor to create a lens that would focus a tsunami, generated by an earthquake near Japan, so that it destroys Los Angeles? For simulations of tsunami propagation, see, e.g., `http://bullard.esc.cam.ac.uk/~taylor/Tsunami.html` .

(d) The height of a tsunami, when it is in the ocean with depth $h_o \sim 4$ km, is only ~ 1 meter or less. Use Eq. (16.19) to show that the tsunami height will increase by a large factor as the tsunami nears the shore.

****

[2]Exercise courtesy David Stevenson.

16.3 Nonlinear Shallow Water Waves and Solitons

In recent decades, *solitons* or solitary waves have been studied intensively in many different areas of physics. However, fluid dynamicists became familiar with them in the nineteenth century. In an oft-quoted pasage, John Scott-Russell (1844) described how he was riding along a narrow canal and watched a boat stop abruptly. This deceleration launched a single smooth pulse of water which he followed on horseback for one or two miles, observing it "rolling on a rate of some eight or nine miles an hour, preserving its original figure some thirty feet long and a foot to a foot and a half in height". This was a soliton – a one dimensional, nonlinear wave with fixed profile traveling with constant speed. Solitons can be observed fairly readily when gravity waves are produced in shallow, narrow channels. We shall use the particular example of a shallow, nonlinear gravity wave to illustrate solitons in general.

16.3.1 Korteweg-de Vries (KdV) Equation

The key to a soliton's behavior is a robust balance between the effects of dispersion and the effects of nonlinearity. When one grafts these two effects onto the wave equation for shallow water waves, then at leading order in the strengths of the dispersion and nonlinearity one gets the *Korteweg-de Vries* (KdV) equation for solitons. Since a completely rigorous derivation of the KdV equation is quite lengthy, we shall content ourselves with a somewhat heuristic derivation that is based on this grafting process, and is designed to emphasize the equation's physical content.

We choose as the dependent variable in our wave equation the height ξ of the water's surface above its quiescent position, and we confine ourselves to a plane wave that propagates in the horizontal x direction so $\xi = \xi(x,t)$.

In the limit of very weak waves, $\xi(x,t)$ is governed by the shallow-water dispersion relation $\omega = \sqrt{gh_o}\,k$, where h_o is the depth of the quiescent water. This dispersion relation implies that $\xi(x,t)$ must satisfy the following elementary wave equation:

$$0 = \frac{\partial^2\xi}{\partial t^2} - gh_o\frac{\partial^2\xi}{\partial x^2} = \left(\frac{\partial}{\partial t} - \sqrt{gh_o}\frac{\partial}{\partial x}\right)\left(\frac{\partial}{\partial t} + \sqrt{gh_o}\frac{\partial}{\partial x}\right)\xi\ . \tag{16.20}$$

In the second expression, we have factored the wave operator into two pieces, one that governs waves propagating rightward, and the other leftward. To simplify our derivation and the final wave equation, we shall confine ourselves to rightward propagating waves, and correspondingly we can simply remove the left-propagation operator from the wave equation, obtaining

$$\frac{\partial\xi}{\partial t} + \sqrt{gh_o}\frac{\partial\xi}{\partial x} = 0\ . \tag{16.21}$$

(Leftward propagating waves are described by this same equation with a change of sign.)

We now graft the effects of dispersion onto this rightward wave equation. The dispersion relation, including the effects of dispersion at leading order, is $\omega = \sqrt{gh_o}\,k(1 - \frac{1}{6}k^2h_o^2)$ [Eq. (16.11)]. Now, this dispersion relation ought to be derivable by assuming a variation $\xi \propto \exp[i(kx - \omega t)]$ and substituting into a generalization of Eq. (16.21) with corrections

that take account of the finite depth of the channel. We will take a short cut and reverse this process to obtain the generalization of Eq. (16.21) from the dispersion relation. The result is

$$\frac{\partial\xi}{\partial t} + \sqrt{gh_o}\,\frac{\partial\xi}{\partial x} = -\frac{1}{6}\sqrt{gh_o}\,h_o^2\frac{\partial^3\xi}{\partial x^3}\ , \tag{16.22}$$

as a direct calculation confirms. This is the "linearized KdV equation". It incorporates weak dispersion associated with the finite depth of the channel but is still a linear equation, only useful for small-amplitude waves.

Now let us set aside the dispersive correction and tackle nonlinearity. For this purpose we return to first principles for waves in very shallow water. Let the height of the surface above the lake bottom be $h = h_o + \xi$. Since the water is very shallow, the horizontal velocity, $v \equiv v_x$, is almost independent of depth (aside from the boundary layer which we ignore); cf. the discussion following Eq. (16.11). The flux of water mass, per unit width of channel, is therefore $\rho h v$ and the mass per unit width is ρh. The law of mass conservation therefore takes the form

$$\frac{\partial h}{\partial t} + \frac{\partial(hv)}{\partial x} = 0\ , \tag{16.23a}$$

where we have canceled the constant density. This equation contains a nonlinearity in the product hv. A second nonlinear equation for h and v can be obtained from the x component of the inviscid Navier-Stokes equation $\partial v/\partial t + v\partial v/\partial x = -(1/\rho)\partial p/\partial x$, with p determined by the weight of the overlying water, $p = g\rho[h(x) - z]$:

$$\frac{\partial v}{\partial t} + v\frac{\partial v}{\partial x} + g\frac{\partial h}{\partial x} = 0\ . \tag{16.23b}$$

Equations (16.23a) and (16.23b) can be combined to obtain

$$\frac{\partial\left(v - 2\sqrt{gh}\right)}{\partial t} + \left(v - \sqrt{gh}\right)\frac{\partial\left(v - 2\sqrt{gh}\right)}{\partial x} = 0\ . \tag{16.23c}$$

This equation shows that the quantity $v - 2\sqrt{gh}$ is constant along characteristics that propagate with speed $v - \sqrt{gh}$. (This constant quantity is a special case of a "Riemann invariant", a concept that we shall study in Chap. 16.) When, as we shall require below, the nonlinearites are modest so h does not differ greatly from h_o, these characteristics propagate leftward, which implies that for rightward propagating waves they begin at early times in undisturbed fluid where $v = 0$ and $h = h_o$. Therefore, the constant value of $v - 2\sqrt{gh}$ is $-2\sqrt{gh_o}$, and correspondingly in regions of disturbed fluid

$$v = 2\left(\sqrt{gh} - \sqrt{gh_o}\right)\ . \tag{16.24}$$

Substituting this into Eq. (16.23a), we obtain

$$\frac{\partial h}{\partial t} + \left(3\sqrt{gh} - 2\sqrt{gh_o}\right)\frac{\partial h}{\partial x} = 0\ . \tag{16.25}$$

We next substitute $\xi = h - h_o$ and expand to second order in ξ to obtain the final form of our wave equation with nonlinearities but no dispersion:

$$\frac{\partial\xi}{\partial t} + \sqrt{gh_o}\frac{\partial\xi}{\partial x} = -\frac{3\xi}{2}\sqrt{\frac{g}{h_o}}\frac{\partial\xi}{\partial x}\ , \tag{16.26}$$

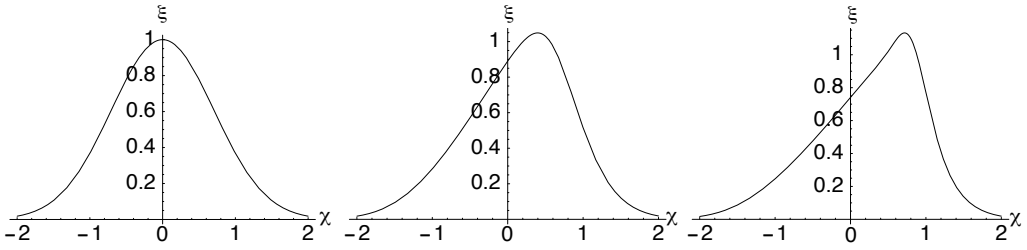

Fig. 16.4: Steepening of a Gaussian wave profile by the nonlinear term in the KdV equation. The increase of wave speed with amplitude causes the leading part of the profile to steepen with time and the trailing part to flatten. In the full KdV equation, this effect can be balanced by the effect of dispersion, which causes the high-frequency Fourier components in the wave to travel slightly slower than the low-frequency components. This allows stable solitons to form.

where the term on the right hand side is the nonlinear correction.

We now have separate dispersive corrections (16.22) and nonlinear corrections (16.26) to the rightward wave equation (16.21). Combining the two corrections into a single equation, we obtain

$$\frac{\partial \xi}{\partial t} + \sqrt{g h_o}\left[\left(1 + \frac{3\xi}{2h_o}\right)\frac{\partial \xi}{\partial x} + \frac{h_o^2}{6}\frac{\partial^3 \xi}{\partial x^3}\right] = 0\ . \tag{16.27}$$

Finally, we substitute

$$\boxed{\chi \equiv x - \sqrt{g h_o}\, t} \tag{16.28}$$

to transform into a frame moving rightward with the speed of small-amplitude gravity waves. The result is the full *Korteweg-deVries* or KdV equation:

$$\boxed{\frac{\partial \xi}{\partial t} + \frac{3}{2}\sqrt{\frac{g}{h_o}}\left(\xi\frac{\partial \xi}{\partial \chi} + \frac{1}{9}h_o^3\frac{\partial^3 \xi}{\partial \chi^3}\right) = 0\ .} \tag{16.29}$$

16.3.2 Physical Effects in the KdV Equation

Before exploring solutions to the KdV equation (16.29), let us consider the physical effects of its nonlinear and dispersive terms. The second, nonlinear term derives from the nonlinearity in the $(\mathbf{v}\cdot\nabla)\mathbf{v}$ term of the Navier-Stokes equation. The effect of this nonlinearity is to steepen the leading edge of a wave profile and flatten the trailing edge (Fig. 16.4.) Another way to understand the effect of this term is to regard it as a nonlinear coupling of linear waves. Since it is nonlinear in the wave amplitude, it can couple together waves with different wave numbers k. For example if we have a purely sinusoidal wave $\propto \exp(ikx)$, then this nonlinearity will lead to the growth of a first harmonic $\propto \exp(2ikx)$. Similarly, when two linear waves with spatial frequencies k, k' are superposed, this term will describe the production of new waves at the sum and difference spatial frequencies. We have already met such wave-wave coupling in our study of nonlinear optics (Chap. 9), and in the route to turbulence for rotating Couette flow (Fig. 14.12), and we shall meet it again in nonlinear plasma physics (Chap. 22).

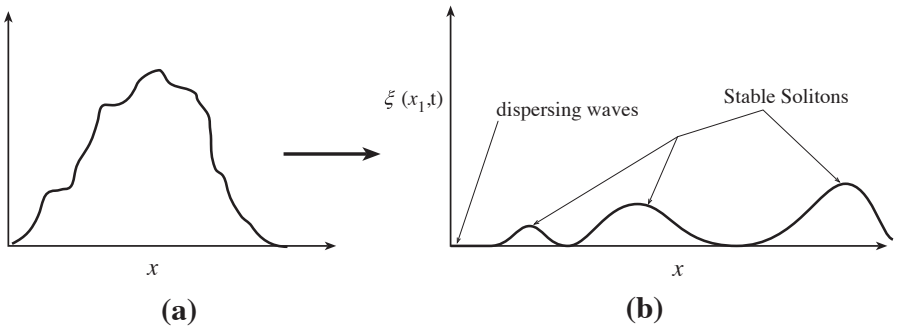

Fig. 16.5: Production of stable solitons out of an irregular initial wave profile.

The third term in (16.29) is linear and is responsible for a weak dispersion of the wave. The higher-frequency Fourier components travel with slower phase velocities than lower-frequency components. This has two effects. One is an overall spreading of a wave in a manner qualitatively familiar from elementary quantum mechanics; cf. Ex. 6.2. For example, in a Gaussian wave packet with width Δx, the range of wave numbers k contributing significantly to the profile is $\Delta k \sim 1/\Delta x$. The spread in the group velocity is then $\sim \Delta k\, \partial^2\omega/\partial k^2 \sim (gh_o)^{1/2} h_o^2\, k\Delta k$ [cf. Eq. (16.11)]. The wave packet will then double in size in a time

$$t_{spread} \sim \frac{\Delta x}{\Delta v_g} \sim \left(\frac{\Delta x}{h_o}\right)^2 \frac{1}{k\sqrt{gh_o}}. \tag{16.30}$$

The second effect is that since the high-frequency components travel somewhat slower than the low-frequency components, there will be a tendency for the profile to become asymmetric with the trailing edge steeper than the leading edge.

Given the opposite effects of these two corrections (nonlinearity makes the wave's leading edge steeper; dispersion reduces its steepness), it should not be too surprising in hindsight that it is possible to find solutions to the KdV equation with constant profile, in which nonlinearity balances dispersion. What is quite surprising, though, is that these solutions, called *solitons*, are very robust and arise naturally out of random initial data. That is to say, if we solve an initial value problem numerically starting with several peaks of random shape and size, then although much of the wave will spread and disappear due to dispersion, we will typically be left with several smooth soliton solutions, as in Fig. 16.5.

16.3.3 Single-Soliton Solution

We can discard some unnecessary algebraic luggage in the KdV equation (16.29) by transforming both independent variables using the substitutions

$$\boxed{\zeta = \frac{\xi}{h_o}\,, \quad \eta = \frac{3\chi}{h_o}\,, \quad \tau = \frac{9}{2}\sqrt{\frac{g}{h_o}}\; t\,.} \tag{16.31}$$

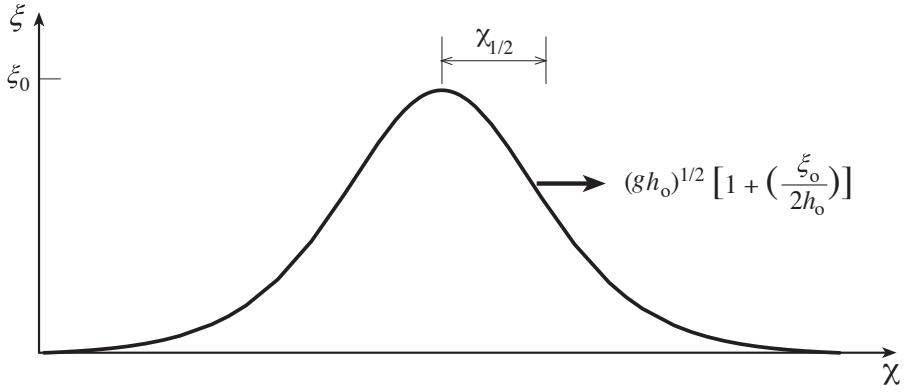

Fig. 16.6: Profile of the single-soliton solution (16.33), (16.31) of the KdV equation. The width $\chi_{1/2}$ is inversely proportional to the square root of the peak height ξ_o.

The KdV equation then becomes

$$\boxed{\frac{\partial\zeta}{\partial\tau}+\zeta\frac{\partial\zeta}{\partial\eta}+\frac{\partial^3\zeta}{\partial\eta^3}=0\ .} \tag{16.32}$$

There are well understood mathematical techniques[3] for solving equations like the KdV equation. However, we shall just quote solutions and explore their properties. The simplest solution to the dimensionless KdV equation (16.32) is

$$\boxed{\zeta=\zeta_0\mathrm{sech}^2\left[\left(\frac{\zeta_0}{12}\right)^{1/2}\left(\eta-\frac{1}{3}\zeta_0\tau\right)\right]\ .} \tag{16.33}$$

This solution describes a one-parameter family of stable solitons. For each such soliton (each ζ_0), the soliton maintains its shape while propagating at speed $d\eta/d\tau=\zeta_0/3$ relative to a weak wave. By transforming to the rest frame of the unperturbed water using Eqs. (16.31) and (16.28), we find for the soliton's speed there;

$$\frac{dx}{dt}=\sqrt{gh_o}\left[1+\left(\frac{\xi_o}{2h_o}\right)\right]\ . \tag{16.34}$$

The first term is the propagation speed of a weak (linear) wave. The second term is the nonlinear correction, proportional to the wave amplitude ξ_o. The half width of the wave may be defined by setting the argument of the hyperbolic secant to unity:

$$\chi_{1/2}=\left(\frac{4h_o^3}{3\xi_o}\right)^{1/2}\ . \tag{16.35}$$

The larger the wave amplitude, the narrower its length and the faster it propagates; cf. Fig. 16.6.

[3]See, for example, Whitham (1974).

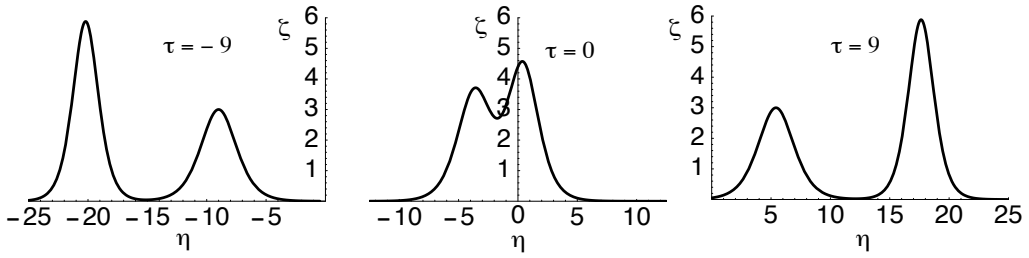

Fig. 16.7: Two-Soliton solution to the dimensionless KdV equation (16.32). This solution describes two waves well separated for $\tau \to -\infty$ that coalesce and then separate producing the original two waves in reverse order as $\tau \to +\infty$. The notation is that of Eq. (16.36); the values of the parameters in that equation are $\eta_1 = \eta_2 = 0$ (so the solitons will be merged at time $\eta = 0$), $\alpha_1 = 1$, $\alpha_2 = 1.4$.

Let us return to Scott-Russell's soliton. Converting to SI units, the speed was about 4 m s^{-1} giving an estimate of the depth of the canal as $h_o \sim 1.6$ m. Using the width $\chi_{1/2} \sim 5$ m, we obtain a peak height $\xi_o \sim 0.25$ m, somewhat smaller than quoted but within the errors allowing for the uncertainty in the definition of the width and an (appropriate) element of hyperbole in the account.

16.3.4 Two-Soliton Solution

One of the most fascinating properties of solitons is the way that two or more waves interact. The expectation, derived from physics experience with weakly coupled normal modes, might be that if we have two well separated solitons propagating in the same direction with the larger wave chasing the smaller wave, then the larger will eventually catch up with the smaller and nonlinear interactions between the two waves will essentially destroy both, leaving behind a single, irregular pulse which will spread and decay after the interaction. However, this is not what happens. Instead, the two waves pass through each other unscathed and unchanged, except that they emerge from the interaction a bit sooner than they would have had they moved with their original speeds during the interaction. See Fig. 16.7. We shall not pause to explain why the two waves survive unscathed, save to remark that there are topological invariants in the solution which must be preserved. However, we can exhibit one such two-soliton solution analytically:

$$\zeta = \frac{\partial^2}{\partial \eta^2}[12 \ln F(\eta, \tau)] \ ,$$
$$\text{where } F = 1 + f_1 + f_2 + \left(\frac{\alpha_2 - \alpha_1}{\alpha_2 + \alpha_1}\right)^2 f_1 f_2 \ ,$$
$$\text{and } f_i = \exp[-\alpha_i(\eta - \eta_i) + \alpha_i^3 \tau] \ ; \tag{16.36}$$

here α_i and η_i are constants. This solution is depicted in Fig. 16.7.

16.3.5 Solitons in Contemporary Physics

Solitons were re-discovered in the 1960's when they were found in numerical plasma simulations. Their topological properties were soon discovered and general methods to generate solutions were derived. Solitons have been isolated in such different subjects as the propagation of magnetic flux in a Josephson junction, elastic waves in anharmonic crystals, quantum field theory (as *instantons*) and classical general relativity (as solitary, nonlinear gravitational waves). Most classical solitons are solutions to one of a relatively small number of nonlinear ordinary differential equations, including the KdV equation, *Burgers' equation* and the *sine-Gordon* equation. Unfortunately it has proved difficult to generalize these equations and their soliton solutions to two and three spatial dimensions.

Just like research into chaos, studies of solitons have taught physicists that nonlinearity need not lead to maximal disorder in physical systems, but instead can create surprisingly stable, ordered structures.

****

EXERCISES

Exercise 16.8 *Example: Breaking of a Dam*
Consider the flow of water along a horizontal channel of constant width after a dam breaks. Sometime after the initial transients have died away, the flow may be described by the nonlinear shallow wave equations (16.23):

$$\frac{\partial h}{\partial t} + \frac{\partial (hv)}{\partial x} = 0 \ , \quad \frac{\partial v}{\partial t} + v\frac{\partial v}{\partial x} + g\frac{\partial h}{\partial x} = 0 \ . \tag{16.37}$$

Here h is the height of the flow, v is the horizontal speed of the flow and x is distance along the channel measured from the location of the dam. Solve for the flow assuming that initially (at $t = 0$) $h = h_o$ for $x < 0$ and $h = 0$ for $x > 0$ (no water). Your solution should have the form shown in Fig. 16.8. What is the speed of the front of the water? [*Hints:* Note that from the parameters of the problem we can construct only one velocity, $\sqrt{gh_o}$ and no length except h_o. It therefore is a reasonable guess that the solution has the self-similar form $h = h_o\ \tilde{h}(\xi)$, $v = \sqrt{gh_o}\ \tilde{v}(\xi)$, where $\tilde{h}$ and $\tilde{v}$ are dimensionless functions of the similarity variable

$$\xi = \frac{x/t}{\sqrt{gh_o}} \ . \tag{16.38}$$

Using this ansatz, convert the partial differential equations (16.37) into a pair of ordinary differential equations which can be solved so as to satisfy the initial conditions.]

Exercise 16.9 *Derivation: Single-Soliton Solution*
Verify that expression (16.33) does indeed satisfy the dimensionless KdV equation (16.32).

Exercise 16.10 *Derivation: Two-Soliton Solution*

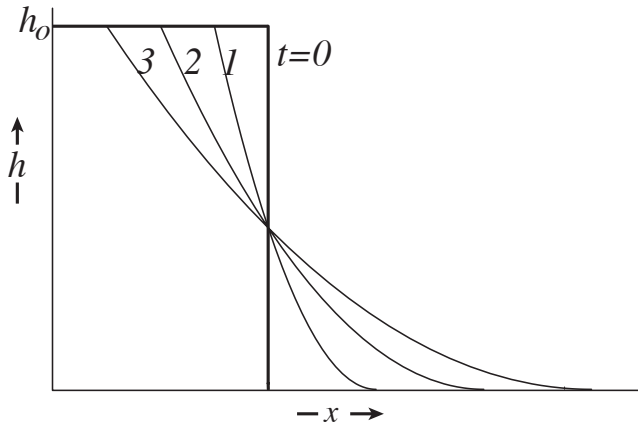

Fig. 16.8: The water's height $h(x,t)$ after a dam breaks.

(a) Verify, using symbolic-manipulation computer software (e.g., Macsyma, Maple or Mathematica) that the two-soliton expression (16.36) satisfies the dimensionless KdV equation. (Warning: Considerable algebraic travail is required to verify this by hand, directly.)

(b) Verify analytically that the two-soliton solution (16.36) has the properties claimed in the text: First consider the solution at early times in the spatial region where $f_1 \sim 1, f_2 \ll 1$. Show that the solution is approximately that of the single-soliton described by Eq. (16.33). Demonstrate that the amplitude is $\zeta_{01} = 3\alpha_1^2$ and find the location of its peak. Repeat the exercise for the second wave and for late times.

(c) Use a computer to follow, numerically, the evolution of this two-soliton solution as time η passes (thereby filling in timesteps between those shown in Fig. 16.7).

****

16.4 Rossby Waves in a Rotating Fluid

In a nearly rigidly rotating fluid, the Coriolis effect (observed in a co-rotating reference frame; Sec. 13.5) provides the restoring force for an unusual type of wave motion called "Rossby waves." These waves are seen in the Earth's oceans and atmosphere.

For a simple example, we consider the sea above a sloping seabed; Fig. 16.9. We assume the unperturbed fluid has vanishing velocity $\mathbf{v} = 0$ in the Earth's rotating frame, and we study weak waves in the sea with oscillating velocity $\mathbf{v}$. (Since the fluid is at rest in the equilibrium state about which we are perturbing, we write the perturbed velocity as $\mathbf{v}$ rather than $\delta\mathbf{v}$.) We assume that the wavelengths are long enough that viscosity is negligible. We shall also, in this case, restrict attention to small-amplitude waves so that nonlinear terms can

be dropped from our dynamical equations. The perturbed Navier-Stokes equation (13.54a) then becomes (after linearization)

$$\frac{\partial \mathbf{v}}{\partial t} + 2\mathbf{\Omega} \times \mathbf{v} = \frac{-\boldsymbol{\nabla}\delta P'}{\rho} \ . \tag{16.39}$$

Here, as in Sec. 13.5, $\delta P'$ is the perturbation in the effective pressure [which includes gravitational and centrifugal effects, $P' = P + \rho\Phi - \frac{1}{2}\rho(\mathbf{\Omega} \times \mathbf{x})^2$]. Taking the curl of Eq. (16.39), we obtain for the time derivative of the waves' vorticity

$$\frac{\partial \boldsymbol{\omega}}{\partial t} = 2(\mathbf{\Omega} \cdot \nabla)\mathbf{v} \ . \tag{16.40}$$

We seek a wave mode in which the horizontal fluid velocity oscillates in the x direction, v_x, $v_y \propto \exp[i(kx - \omega t)]$, and is independent of z in accord with the Taylor-Proudman theorem (Sec. 13.5.3):

$$v_x \text{ and } v_y \propto \exp[i(kx - \omega t)] \ , \quad \frac{\partial v_x}{\partial z} = \frac{\partial v_y}{\partial z} = 0 \ . \tag{16.41}$$

The only allowed vertical variation is in the vertical velocity v_z, and differentiating $\boldsymbol{\nabla} \cdot \mathbf{v} = 0$ with respect to z, we obtain

$$\frac{\partial^2 v_z}{\partial z^2} = 0 \ . \tag{16.42}$$

The vertical velocity therefore varies linearly between the surface and the sea floor. Now, one boundary condition is that the vertical velocity must vanish at the surface. The other is that, at the seafloor $z = -h$, we must have $v_z(-h) = -\alpha v_y(x)$, where α is the tangent of the angle of inclination of the sea floor. The solution to Eq. (16.42) satisfying these boundary conditions is

$$v_z = \frac{\alpha z}{h} v_y \ . \tag{16.43}$$

Taking the vertical component of Eq. (16.40) and evaluating $\omega_z = v_{y,x} - v_{x,y} = ikv_y$, we obtain

$$\omega k v_y = 2\Omega \frac{\partial v_z}{\partial z} = \frac{2\Omega\alpha v_y}{h} \ . \tag{16.44}$$

The dispersion relation therefore has the quite unusual form

$$\boxed{\omega k = \frac{2\Omega\alpha}{h} \ .} \tag{16.45}$$

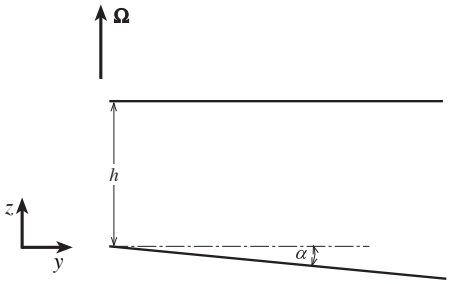

Fig. 16.9: Geometry of ocean for Rossby waves.

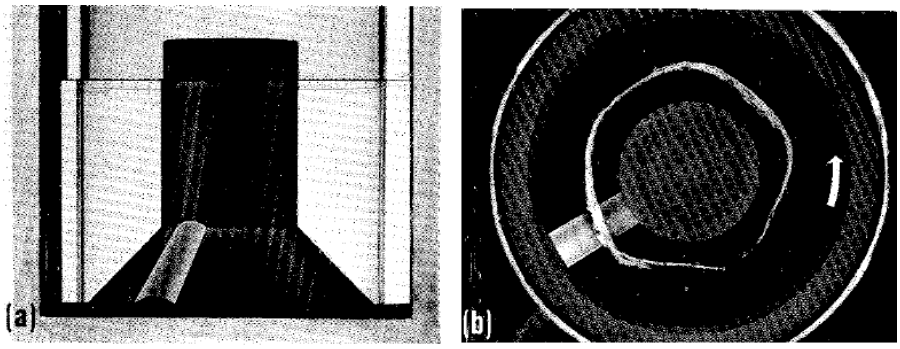

Fig. 16.10: Rossby Waves in a Rotating cylinder with sloping bottom.

Rossby waves have interesting properties: They can only propagate in one direction—parallel to the intersection of the sea floor with the horizontal (our $\mathbf{e}_x$ direction). Their phase velocity $\mathbf{V}_{\rm ph}$ and group velocity $\mathbf{V}_g$ are equal in magnitude but in opposite directions,

$$\mathbf{V}_{\rm ph} = -\mathbf{V}_g = \frac{2\Omega\alpha}{k^2 h}\mathbf{e}_x \ . \tag{16.46}$$

If we use $\boldsymbol{\nabla}\cdot\mathbf{v} = 0$, we discover that the two components of horizontal velocity are in quadrature, $v_x = i\alpha v_y/kh$. This means that, when seen from above, the fluid circulates with the opposite sense to the angular velocity Ω.

Rossby waves plays an important role in the circulation of the earth's oceans; see, e.g., Chelton and Schlax (1996). A variant of these Rossby waves in air can be seen as undulations in the atmosphere's jet stream produced when the stream goes over a sloping terrain such as that of the Rocky Mountains; and another variant in neutron stars generates gravitational waves (ripples of spacetime curvature) that are a promising source for ground-based detectors such as LIGO.

****

EXERCISES

Exercise 16.11 *Example: Rossby Waves in a Cylndrical Tank with Sloping Bottom*

In the film *Rotating Fluids* by David Fultz (1969), about 20 minutes 40 seconds into the film, an experiment is described in which Rossby waves are excited in a rotating cylindrical tank with inner and outer vertical walls and a sloping bottom. Figure 16.11(a) is a photograph of the tank from the side, showing its bottom which slopes upward toward the center, and a bump on the bottom which generates the Rossby waves. The tank is filled with water, then set into rotation with an angular velocity Ω; the water is given time to settle down into rigid rotation with the cylinder. Then the cylinder's angular velocity is reduced by a small amount, so the water is rotating at angular velocity $\Delta\Omega \ll \Omega$ relative to the cylinder. As the water passes over the hump on the tank bottom, the hump generates Rossby waves. Those waves are made visible by injecting dye at a fixed radius, through a syringe attached to the tank. Figure 16.11(b) is a photograph of the dye trace as seen looking down on the tank

from above. If there were no Rossby waves present, the trace would be circular. The Rossby waves make it pentagonal. In this exercise you will work out the details of the Rossby waves, explore their physics, and explain the shape of the trace.

Because the slope of the bottom is cylindrical rather than planar, this is somewhat different from the situation in the text (Fig. 16.9). However, we can deduce the details of the waves in this cylindrical case from those for the planar case by geometric optics considerations, making modest errors because the wavelength of the waves is not all that small compared to the circumference around the tank.

(a) Show that the rays along which the waves propagate are circles centered on the tank's symmetry axis.

(b) Focus on the ray that is half way between the inner and outer walls of the tank. Let its radius be a and the depth of the water there be h, and the slope angle of the tank floor be α. Introduce quasi-Cartesian coordinates $x = a\phi$, $y = -\varpi$, where $\{\varpi, \phi, z\}$ are cylindrical coordinates. By translating the Cartesian-coordinate waves of the text into quasi-Cartesian coordinates and noting that five wavelengths must fit into the circumference around the cylinder, show that the velocity field has the form $v_\varpi, v_\phi, v_z \propto e^{i(10\pi\phi+\omega t)}$ and deduce the ratios of the three components of velocity to each other. This solution has nonzero radial velocity at the walls — a warning that edge effects will modify the waves somewhat. This analysis ignores those edge effects.

(c) Because the waves are generated by the ridge on the bottom of the tank, the wave pattern must remain at rest relative to that ridge, which means it must rotate relative to the fluid's frame with the angular velocity $d\phi/dt = -\Delta\Omega$. From the waves' dispersion relation deduce $\Delta\Omega/\Omega$, the fractional slowdown of the tank that had to be imposed, in order to generate the observed pentagonal wave.

(d) Compute the displacement field $\delta\mathbf{x}(\varpi, \phi, z, t)$ of a fluid element whose undisplaced location (in the rigidly rotating cylindrical coordinates) is (ϖ, ϕ, z). Explain the pentagonal shape of the movie's dye lines in terms of this displacement field.

(e) Compute the wave's vertical vorticity field ω_z (relative to the rigidly rotating flow), and show that as a fluid element moves, and the vertical vortex line through it shortens or lengths due to the changing water depth, ω_z changes proportionally to the vortex line's length (as it must).

****

16.5 Sound Waves

So far, our discussion of fluid dynamics has mostly been concerned with flows sufficiently slow that the density can be treated as constant. We now introduce the effects of compressibility by discussing sound waves (in a *non*-rotating reference frame). Sound waves are prototypical

scalar waves and therefore are simpler in many respects than vector electromagnetic waves and tensor gravitational waves.

For a sound wave in the small-amplitude limit, we linearize the Euler and continuity (mass conservation) equations to obtain

$$\rho\frac{\partial \mathbf{v}}{\partial t} = -\boldsymbol{\nabla}\delta P \ , \tag{16.47a}$$

$$\frac{\partial \delta\rho}{\partial t} = -\rho\boldsymbol{\nabla}\cdot\mathbf{v} \ . \tag{16.47b}$$

As the flow is irrotational (vanishing vorticity before the wave arrives implies vanishing vorticity as it is passing), we can write the fluid velocity as the gradient of a velocity potential:

$$\boxed{\mathbf{v} = \boldsymbol{\nabla}\psi \ .} \tag{16.48a}$$

Inserting this into Eq. (16.47a) and integrating spatially (with ρ regarded as constant since its perturbation would give a second-order term), we obtain

$$\boxed{\delta P = -\rho\frac{\partial \psi}{\partial t} \ .} \tag{16.48b}$$

Setting $\delta\rho = (\partial\rho/\partial P)_s \delta P$ in Eq. (16.47b) (with the derivative performed at constant entropy s because there generally will not be enough time in a single wave period for heat to cross a wavelength), and expressing δP and $\boldsymbol{\nabla}\mathbf{v}$ in terms of the velocity potential [Eqs. (16.48a) and (16.48b)], we obtain the dispersion-free wave equation

$$\boxed{\nabla^2\psi = \frac{1}{c^2}\frac{\partial^2\psi}{\partial t^2} \ .} \tag{16.48c}$$

Here

$$\boxed{c = \left[\left(\frac{\partial P}{\partial \rho}\right)_s\right]^{1/2}} \tag{16.48d}$$

is the adiabatic sound speed. For a perfect gas its value is $c = (\gamma P/\rho)^{1/2}$ where γ is the ratio of specific heats. The sound speed in air at 20°C is 340m s^{-1}. In water under atmospheric conditions, it is about 1.5km s^{-1} (not much different from sound speeds in solids).

The general solution of the wave equation (16.48c) for plane sound waves propagating in the $\pm x$ directions is

$$\psi = f_1(x - ct) + f_2(x + ct) \ , \tag{16.49}$$

where f_1, f_2 are arbitrary functions.

16.5.1 Wave Energy

We shall use sound waves to illustrate how waves carry energy. The fluid's energy density is $U = (\frac{1}{2}v^2 + u)\rho$ [Table 12.1 with $\Phi = 0$]. The first term is the fluid's kinetic energy;

the second, its internal energy. The internal energy density can be evaluated by a Taylor expansion in the wave's density perturbation:

$$u\rho = [u\rho] + \left[\left(\frac{\partial(u\rho)}{\partial\rho}\right)_s\right]\delta\rho + \frac{1}{2}\left[\left(\frac{\partial^2(u\rho)}{\partial\rho^2}\right)_s\right]\delta\rho^2 \tag{16.50}$$

where the three coefficients in brackets [] are evaluated at the equilibrium density. The first term in Eq. (16.50) is the energy of the background fluid, so we shall drop it. The second term will average to zero over a wave period, so we shall also drop it. The third term can be simplified using the first law of thermodynamics in the form $du = Tds - Pd(1/\rho)$ (which implies $[\partial(u\rho)/\partial\rho]_s = u + P/\rho$), followed by the definition $h = u + P/\rho$ of enthalpy density, followed by the first law in the form $dh = Tds + dP/\rho$, followed by expression (16.48d) for the speed of sound. The result is

$$\left(\frac{\partial^2(u\rho)}{\partial\rho^2}\right)_s = \left(\frac{\partial h}{\partial\rho}\right)_s = \frac{c^2}{\rho}\,. \tag{16.51}$$

Inserting this into the third term of (16.50) and averaging over a wave period and wavelength, we obtain for the wave energy per unit volume

$$\varepsilon = \frac{1}{2}\rho\overline{v^2} + \frac{c^2}{2\rho}\overline{\delta\rho^2} = \frac{1}{2}\rho\left[\overline{(\boldsymbol{\nabla}\psi)^2 + \frac{1}{c^2}\left(\frac{\partial\psi}{\partial t}\right)^2}\right] = \rho\overline{(\boldsymbol{\nabla}\psi)^2}\,. \tag{16.52}$$

In the second equality we have used $\mathbf{v} = \boldsymbol{\nabla}\psi$ [Eq. (16.48a)] and $\delta\rho = (\rho/c^2)\partial\psi/\partial t$ [from $\delta\rho = (\partial\rho/\partial P)_s\delta P = \delta P/c^2$ and Eq. (16.48b)]; the third equality can be deduced by multiplying the wave equation (16.48c) by ψ and averaging. Thus, there is equipartition of energy between the kinetic and internal energy terms.

The energy flux is $\mathbf{F} = (\frac{1}{2}v^2 + h)\rho\mathbf{v}$ [Table 12.1 with $\Phi = 0$]. The kinetic energy flux (first term) is third order in the velocity perturbation and therefore vanishes on average. For a sound wave, the internal energy flux (second term) can be brought into a more useful form by expanding the enthalpy per unit mass:

$$h = [h] + \left[\left(\frac{\partial h}{\partial P}\right)_s\right]\delta P = [h] + \frac{\delta P}{\rho}\,. \tag{16.53}$$

Here we have used the first law of thermodynamics $dh = Tds + (1/\rho)dP$ and adiabaticity of the perturbation, $s =$constant; and the terms in square brackets are unperturbed quantities. Inserting this into $\mathbf{F} = h\rho\mathbf{v}$ and expressing δP and $\mathbf{v}$ in terms of the velocity potential [Eqs. (16.48a) and (16.48b)], and averaging over a wave period and wavelength, we obtain for the energy flux

$$\mathbf{F} = \overline{\rho h\mathbf{v}} = \overline{\delta P\,\mathbf{v}} = -\rho\overline{\left(\frac{\partial\psi}{\partial t}\right)\boldsymbol{\nabla}\psi}\,. \tag{16.54}$$

This equation and Eq. (16.52) are a special case of the scalar-wave energy flux and energy density discussed in Sec. 6.3.1 and Ex. 6.9 [Eqs. (6.18)].

For a locally plane wave with $\psi = \psi_o\cos(\mathbf{k}\cdot\mathbf{x} - \omega t + \varphi)$ (where φ is an arbitrary phase), the energy density (16.52) is $\varepsilon = \frac{1}{2}\rho\psi_o^2k^2$, and the energy flux (16.54) is $\mathbf{F} = \frac{1}{2}\rho\psi_o^2\omega\mathbf{k}$. Since,

for this dispersion-free wave, the phase and group velocities are both $\mathbf{V} = (\omega/k)\hat{\mathbf{k}} = c\hat{\mathbf{k}}$ (where $\hat{\mathbf{k}} = \mathbf{k}/k$ is the unit vector pointing in the wave-propagation direction), the energy density and flux are related by

$$\boxed{\mathbf{F} = \varepsilon\mathbf{V} = \varepsilon c\hat{\mathbf{k}} \; .} \tag{16.55}$$

The energy flux is therefore the product of the energy density and the wave velocity, as we might have anticipated.

When studying dispersive waves in plasmas (Chaps. 20 and 22) we shall return to the issue of energy transport, and shall see that just as information in waves is carried at the group velocity, not the phase velocity, so energy is also carried at the group velocity.

In Sec. 6.3.1 we used the above equations for the sound-wave energy density ε (there denoted u) and flux $\mathbf{F}$ to illustrate, via geometric-optics considerations, the behavior of wave energy in an inhomogeneous, time-varying medium.

The energy flux carried by sound is conventionally measured in dB (decibels). The flux in decibels, $F_{\rm dB}$, is related to the flux F in W m^{-2} by

$$\boxed{F_{\rm dB} = 120 + 10\log_{10}(F) \; .} \tag{16.56}$$

Sound that is barely audible is about 1 dB. Normal conversation is about 50-60 dB. Jet aircraft and rock concerts can cause exposure to more than 120 dB with consequent damage to the ear.

16.5.2 Sound Generation

So far in this book, we have been concerned with describing how different types of waves propagate. It is also important to understand how they are emitted. We now outline some aspects of the theory of sound generation.

The reader should be familiar with the theory of electromagnetic wave emission. There, one considers a localised region containing moving charges and consequently variable currents. The source can be described as a sum over electric and magnetic multipoles, and each multipole in the source produces a characteristic angular variation of the distant radiation field. The radiation-field amplitude decays inversely with distance from the source and so the Poynting flux varies with the inverse square of the distance. Integrating over a large sphere gives the total power radiated by the source, broken down into the power radiated by each multipolar component. When the reduced wavelength $\lambda\!\!\!^{-} = 1/k$ of the waves is small compared to the source (a situation referred to as *slow motion* since the source's charges then generally move slowly compared to the speed of light), the most powerful radiating multipole is the electric dipole $\mathbf{d}(t)$. The dipole's average emitted power is given by the Larmor formula

$$\mathcal{P} = \frac{\overline{\ddot{\mathbf{d}}^2}}{6\pi\epsilon_0 c^3} \; , \tag{16.57}$$

where $\ddot{\mathbf{d}}$ is the second time derivative of $\mathbf{d}$, the bar denotes a time average, and c is the speed of light, not sound.

This same procedure can be followed when describing sound generation. However, as we are dealing with a scalar wave, sound can have a monopolar source. As an pedagogical

example, let us set a small, spherical, elastic ball, surrounded by fluid, into radial oscillation (not necessarily sinusoidal) with oscillation frequencies of order ω, so the emitted waves have reduced wavelengths of order $\lambda = c/\omega$. Let the surface of the ball have radius $a + \xi(t)$, and impose the *slow-motion* and *small-amplitude* conditions that

$$\lambda\!\!\!^{-} \gg a \gg |\xi| \; . \tag{16.58}$$

As the waves will be spherical, the relevant outgoing-wave solution of the wave equation (16.48c) is

$$\psi = \frac{f(t - r/c)}{r} \; , \tag{16.59}$$

where f is a function to be determined. Since the fluid's velocity at the ball's surface must match that of the ball, we have (to first order in $\mathbf{v}$ and ψ)

$$\dot{\xi}\mathbf{e}_r = \mathbf{v}(a,t) = \boldsymbol{\nabla}\psi \simeq -\frac{f(t - a/c)}{a^2}\mathbf{e}_r \simeq -\frac{f(t)}{a^2}\mathbf{e}_r \; , \tag{16.60}$$

where in the third equality we have used the slow-motion condition. Solving for $f(t)$ and inserting into Eq. (16.59), we see that

$$\psi(r,t) = -\frac{a^2\dot{\xi}(t - r/c)}{r} \; . \tag{16.61}$$

It is customary to express the radial velocity perturbation v in terms of an oscillating fluid *monopole moment*

$$\boxed{q = 4\pi\rho a^2\dot{\xi} \; .} \tag{16.62}$$

Physically this is the total radial discharge of air mass (i.e. mass per unit time) crossing an imaginary fixed spherical surface of radius slightly larger than that of the oscillating ball. In terms of q we have $\dot{\xi}(t) = q(t)/4\pi\rho a^2$. Using this and Eq. (16.61), we compute for the power radiated as sound waves [Eq. (16.54) integrated over a sphere centered on the ball]

$$\boxed{\mathcal{P} = \frac{\overline{\ddot{q}^2}}{4\pi\rho c} \; .} \tag{16.63}$$

Note that the power is inversely proportional to the signal speed. This is characteristic of monopolar emission and in contrast to the inverse cube variation for dipolar emission [Eq. (16.57)].

The emission of monopolar waves requires that the volume of the emitting solid body oscillate. When the solid simply oscillates without changing its volume, for example the reed on a musical instrument, dipolar emission should generally dominate. We can think of this as two monopoles of size a in antiphase separated by some displacement $b \sim a$. The velocity potential in the far field is then the sum of two monopolar contributions, which almost cancel. Making a Taylor expansion, we obtain

$$\frac{\psi_{\rm dipole}}{\psi_{\rm monopole}} \sim \frac{b}{\lambda\!\!\!^{-}} \sim \frac{\omega b}{c} \; , \tag{16.64}$$

where ω and $\lambda\!\!\!^{-}$ are the characteristic magnitudes of the angular frequency and reduced wavelength of the waves (which we have not assumed to be precisely sinusoidal).

This reduction of ψ by the slow-motion factor $\omega b/c$ implies that the dipolar power emission is weaker than monopolar power by a factor $\sim (\omega b/c)^2$ for similar frequencies and amplitudes of motion. However, to emit dipole radiation, momentum must be given to and removed from the fluid. In other words the fluid must be forced by a solid body. In the absence of such a solid body, the lowest multipole that can be radiated effectively is quadrupolar radiation, which is weaker by yet one more factor of $(\omega b/c)^2$.

These considerations are important to understanding how noise is produced by the intense turbulence created by jet engines, especially close to airports. We expect that the sound emitted by the free turbulence in the wake just behind the engine will be quadrupolar and will be dominated by emission from the largest (and hence fastest) turbulent eddies. [See the discussion of turbulent eddies in Sec. 14.3.4.] Denote by ℓ and v_ℓ the size and turnover speed of these largest eddies. Then the characteristic size of the sound's source will be $a \sim b \sim \ell$, the mass discharge will be $q \sim \rho\ell^2 v_\ell$, the characteristic frequency will be $\omega \sim v_\ell/\ell$, the reduced wavelength of the sound waves will be $\lambda\!\!\!^{-} = c/\omega \sim \ell c/v_\ell$, and the slow-motion parameter will be $b/\lambda\!\!\!^{-} \sim \omega b/c \sim v_\ell/c$. The quadrupolar power radiated per unit volume [Eq. (16.63) divided by the volume ℓ^3 of an eddy and reduced by $\sim (b\omega/c)^4$] will therefore be

$$\frac{d\mathcal{P}}{d^3x} \sim \rho \frac{v_\ell^3}{\ell}\left(\frac{v_\ell}{c}\right)^5 , \tag{16.65}$$

and this power will be concentrated around frequency $\omega \sim v_\ell/\ell$. For air of fixed sound speed and length scale, and for which the largest eddy speed is proportional to some characteristic speed V (e.g. the average speed of the air leaving the engine), the sound generation increases proportional to the eighth power of the Mach number $M = V/c$. This is known as Lighthill's law. The implications for the design of jet engines should be obvious.

16.5.3 T2 Radiation Reaction, Runaway Solutions, and Matched Asymptotic Expansions[4]

Let us return to our idealized example of sound waves produced by a radially oscillating, spherical ball. We shall use this example to illustrate several deep issues in theoretical physics: the *radiation-reaction force* that acts back on a source due to its emission of radiation, a spurious *runaway solution* to the source's equation of motion caused by the radiation-reaction force, and *matched asymptotic expansions*, a mathematical technique for solving field equations when there are two different regions of space in which the equations have rather different behaviors. We shall meet these concepts again, in a rather more complicated way, in Chap. 26, when studying the radiation reaction force caused by emission of gravitational waves.

For our oscillating ball, the two different regions of space that we shall match to each other are the *near zone*, $r \ll \lambda\!\!\!^{-}$, and the *wave zone*, $r \gtrsim \lambda\!\!\!^{-}$.

We consider, first, the near zone, and we redo, from a new point of view, the analysis of the matching of the near-zone fluid velocity to the ball's surface velocity and the computation

[4]Our treatment is based on Burke (1970).

of the pressure perturbation. Because the region near the ball is small compared to $\lambda\!\!\!^{-}$ and the fluid speeds are small compared to c, the flow is very nearly incompressible $\boldsymbol{\nabla}\cdot\mathbf{v} = \nabla^2\psi = 0$; cf. the discussion of conditions for incompressibility in Sec. 12.6. [The near-zone equation $\nabla^2\psi = 0$ is analogous to $\nabla^2\Phi = 0$ for the Newtonian gravitational potential in the weak-gravity near zone of a gravitational-wave source (Chap. 26).]

The general monopolar (spherical) solution to $\nabla^2\psi = 0$ is

$$\psi = \frac{A(t)}{r} + B(t) \; . \tag{16.66}$$

Matching the fluid's radial velocity $v = \partial\psi/\partial r = -A/r^2$ at $r = a$ to the ball's radial velocity $\dot{\xi}$, we obtain

$$A(t) = -a^2\dot{\xi}(t) \; . \tag{16.67}$$

From the point of view of near-zone physics there is no mechanism for generating a nonzero spatially constant term $B(t)$ in ψ [Eq. (16.66)], so if one were unaware of the emitted waves and their action back on the source, one would be inclined to set this $B(t)$ to zero. [This is analogous to a Newtonian physicist who would be inclined to write the quadrupolar contribution to an axisymmetric source's external gravitational field in the form $\Phi = P_2(\cos\theta)[A(t)r^{-3} + B(t)r^2]$ and then, being unaware of gravitational waves and their action back on the source, would set $B(t)$ to zero; see Chap. 26]. Taking this near-zone point of view, with $B = 0$, we infer that the fluid's pressure perturbation acting on the ball's surface is

$$\delta P = -\rho\frac{\partial\psi(a,t)}{\partial t} = -\rho\frac{\dot{A}}{a} = \rho a\ddot{\xi} \; . \tag{16.68}$$

The motion $\xi(t)$ of the ball's surface is controlled by the elastic restoring forces in its interior and the fluid pressure perturbation δP on its surface. In the absence of δP the surface would oscillate sinusoidally with some angular frequency ω_o, so $\ddot{\xi} + \omega_o^2\xi = 0$. The pressure will modify this to

$$m(\ddot{\xi} + \omega_o^2\xi) = -4\pi a^2\delta P \; , \tag{16.69}$$

where m is an effective mass, roughly equal to the ball's true mass, and the right hand side is the integral of the radial component of the pressure perturbation force over the sphere's surface. Inserting the near-zone viewpoint's pressure perturbation (16.68), we obtain

$$(m + 4\pi a^3\rho)\ddot{\xi} + m\omega_o^2\xi = 0 \; . \tag{16.70}$$

Evidently, the fluid increases the ball's effective inertial mass (it *loads* additional mass onto the ball), and thereby reduces its frequency of oscillation to

$$\omega = \frac{\omega_o}{\sqrt{1+\kappa}} \; , \quad \text{where } \kappa = \frac{4\pi a^3\rho}{m} \tag{16.71}$$

is a measure of the coupling strength between the ball and the fluid. In terms of this loaded frequency the equation of motion becomes

$$\ddot{\xi} + \omega^2\xi = 0 \; . \tag{16.72}$$

This near-zone viewpoint is not quite correct, just as the standard Newtonian viewpoint is not quite correct for the near-zone gravity of a gravitational-wave source (Chap. 26). To improve on this viewpoint, we temporarily move out into the wave zone and identify the general, outgoing-wave solution to the sound wave equation,

$$\psi = \frac{f(t - \epsilon r/c)}{r} \tag{16.73}$$

[Eq. (16.59)]. Here f is a function to be determined by matching to the near zone, and ϵ is a parameter that has been inserted to trace the influence of the outgoing-wave boundary condition. For outgoing waves (the real, physical, situation), $\epsilon = +1$; if the waves were ingoing, we would have $\epsilon = -1$.

This wave-zone solution remains valid down into the near zone. In the near zone we can perform a slow-motion expansion to bring it into the same form as the near-zone velocity potential (16.66):

$$\psi = \frac{f(t)}{r} - \epsilon\frac{\dot{f}(t)}{c} + \dots \ . \tag{16.74}$$

The second term is sensitive to whether the waves are outgoing or ingoing and thus must ultimately be responsible for the radiation reaction force that acts back on the oscillating ball; for this reason we will call it the *radiation-reaction potential*.

Equating the first term of this ψ to the first term of (16.66) and using the value (16.67) of $A(t)$ obtained by matching the fluid velocity to the ball velocity, we obtain

$$f(t) = A(t) = -a^2\dot{\xi}(t) \ . \tag{16.75}$$

This equation tells us that the wave field $f(t - r/c)/r$ generated by the ball's surface displacement $\xi(t)$ is given by $\psi = -a^2\dot{\xi}(t - r/c)/r$ [Eq. (16.61)] — the result we derived more quickly in the previous section. *We can regard Eq. (16.75) as matching the near-zone solution outward onto the wave-zone solution to determine the wave field as a function of the source's motion.*

Equating the second term of Eq. (16.74) to the second term of the near-zone velocity potential (16.66) we obtain

$$B(t) = -\epsilon\frac{\dot{f}(t)}{c} = \epsilon\frac{a^2}{c}\ddot{\xi}(t) \ . \tag{16.76}$$

This is the term in the near-zone velocity potential $\psi = A/r + B$ that will be responsible for radiation reaction. *We can regard this radiation reaction potential $\psi^{\rm RR} = B(t)$ as having been generated by matching the wave zone's outgoing (or ingoing) wave field back into the near zone.*

This pair of matchings, outward then inward, is a special, almost trivial example of the technique of *matched asymptotic expansions* — a technique developed by applied mathematicians to deal with much more complicated matching problems than this one (see e.g. Cole, 1968).

The radiation-reaction potential $\psi^{\rm RR} = B(t) = \epsilon(a^2/c)\ddot{\xi}(t)$ gives rise to a radiation-reaction contribution to the pressure on the ball's surface $\delta P^{\rm RR} = -\rho\dot{\psi}^{\rm RR} = -\epsilon(\rho a^2/c)\dddot{\xi}$. Inserting this into the equation of motion (16.69) along with the loading pressure (16.68)

and performing the same algebra as before, we get the following radiation-reaction-modified form of Eq. (16.72):

$$\boxed{\ddot{\xi} + \omega^2 \xi = \epsilon\tau \dddot{\xi}\ ,} \quad \text{where } \tau = \frac{\kappa}{1+\kappa}\frac{a}{c} \tag{16.77}$$

is less than the fluid's sound travel time to cross the ball's radius, a/c. The term $\epsilon\tau\dddot{\xi}$ in the equation of motion is the ball's *radiation-reaction acceleration*, as we see from the fact that it would change sign if we switched from outgoing waves, $\epsilon = +1$, to ingoing waves, $\epsilon = -1$.

In the absence of radiation reaction, the ball's surface oscillates sinusoidally in time, $\xi = e^{\pm i\omega t}$. The radiation reaction term produces a weak damping of these oscillations:

$$\boxed{\xi \propto e^{\pm i\omega t} e^{-\sigma t}\ , \quad \text{where } \sigma = \frac{1}{2}\epsilon(\omega\tau)\omega} \tag{16.78}$$

is the radiation-reaction-induced damping rate. Note that in order of magnitude the ratio of the damping rate to the oscillation frequency is $\sigma/\omega = \omega\tau \lesssim \omega a/c = a/\lambda\!\!\!^{-}$, which is small compared to unity by virtue of the slow-motion assumption. If the waves were ingoing rather than outgoing, $\epsilon = -1$, the fluid's oscillations would grow. In either case, outgoing waves or ingoing waves, the radiation reaction force removes energy from the ball or adds it at the same rate as the sound waves carry energy off or bring it in. The total energy, wave plus ball, is conserved.

Expression (16.78) is two linearly independent solutions to the equation of motion (16.77) — one with the sign + and the other −. Since this equation of motion has been made third order by the radiation-reaction term, there must be a third independent solution. It is easy to see that, up to a tiny fractional correction, that third solution is

$$\xi \propto e^{\epsilon t/\tau}\ . \tag{16.79}$$

For outgoing waves, $\epsilon = +1$, this solution grows exponentially in time, on an extremely rapid timescale $\tau \lesssim a/c$; it is called a *runaway solution*.

Such runaway solutions are ubiquitous in equations of motion with radiation reaction. For example, a computation of the electromagnetic radiation reaction on a small, classical, electrically charged, spherical particle gives the Abraham-Lorentz equation of motion

$$m(\ddot{\mathbf{x}} - \tau\dddot{\mathbf{x}}) = \mathbf{F}_{\rm ext} \tag{16.80}$$

(Rorlich 1965; Sec. 16.2 of Jackson 1999). Here $\mathbf{x}(t)$ is the the particle's world line, $\mathbf{F}_{\rm ext}$ is the external force that causes the particle to accelerate, and the particle's inertial mass m includes an electrostatic contribution analogous to $4\pi a^3\rho$ in our fluid problem. The timescale τ, like that in our fluid problem, is very short, and when the external force is absent, there is a runaway solution $\mathbf{x} \propto e^{t/\tau}$.

Much human heat and confusion were generated, in the the early and mid 20th century, over these runaway solutions (see, e.g., Rorlich 1965). For our simple model problem, little heat or confusion need be expended. One can easily verify that the runaway solution (16.79) violates the slow-motion assumption $a/\lambda\!\!\!^{-} \ll 1$ that underlies our derivation of the radiation reaction acceleration. It therefore is a spurious solution.

Our model problem is sufficiently simple that one can dig deeper into it and learn that the runaway solution arises from the slow-motion approximation trying to reproduce a genuine, rapidly damped solution and getting the sign of the damping wrong (Ex. 16.14 and Burke 1970).

****

EXERCISES

Exercise 16.12 *Problem: Aerodynamic Sound Generation*
Consider the emission of quadrupolar sound waves by a Kolmogorov spectrum of free turbulence (Sec. 14.3.4). Show that the power radiated per unit frequency interval has a spectrum

$$\mathcal{P}_\omega \propto \omega^{-7/2} \ .$$

Also show that the total power radiated is roughly a fraction M^5 of the power dissipated in the turbulence, where M is the Mach number.

Exercise 16.13 *Problem: Energy Conservation for Radially Oscillating Ball Plus Sound Waves*
For the radially oscillating ball as analyzed in Sec. 16.5.3, verify that the radiation reaction acceleration removes energy from the ball, plus the fluid loaded onto it, at the same rate as the gravitational waves carry energy away.

Exercise 16.14 *Problem: Radiation Reaction Without the Slow Motion Approximation*
Redo the computation of radiation reaction for a radially oscillating ball immersed in a fluid, without imposing the slow-motion assumption and approximation. Thereby obtain the following coupled equations for the radial displacement $\xi(t)$ of the ball's surface and the function $\Phi(t) \equiv a^{-2} f(t - \epsilon a/c)$, where $\psi = r^{-1} f(t - \epsilon r/c)$ is the sound-wave field:

$$\ddot{\xi} + \omega_o^2 \xi = \kappa \dot{\Phi} \ , \quad \dot{\xi} = -\Phi - \epsilon(a/c)\dot{\Phi} \ . \tag{16.81}$$

Show that in the slow-motion regime, this equation of motion has two weakly damped solutions of the same form (16.78) as we derived using the slow-motion approximation, and one rapidly damped solution $\xi \propto \exp(-\epsilon\kappa/\tau)$. Burke (1970) shows that the runaway solution (16.79) obtained using the slow-motion approximation is caused by that approximation's futile attempt to reproduce this genuine, rapidly damped solution (16.81).

Exercise 16.15 *Problem: Sound Waves from a Ball Undergoing Quadrupolar Oscillations*
Repeat the analysis of gravitational wave emission, radiation reaction, and energy conservation, as given in Sec. 16.5.3 and Ex. 16.13, for axisymmetric, quadrupolar oscillations of an elastic ball, $r_{\rm ball} = a + \xi(t) P_2(\cos\theta)$.

Comment: Since the lowest multipolar order for gravitational waves is quadrupolar, this exercise is closer to the analogous problem of gravitational wave emission than the monopolar analysis in the text.

Hint: If ω is the frequency of the ball's oscillations, then the sound waves have the form

$$\psi = K\Re\left[e^{-i\omega t}\left(\frac{n_2(\omega r/c) - i\epsilon j_2(\omega r/c)}{r}\right)\right] , \tag{16.82}$$

where K is a constant, $\Re(X)$ is the real part of X, ϵ is $+1$ for outgoing waves and -1 for ingoing waves, and j_2 and n_2 are the spherical Bessel and spherical Neuman functions of order 2. In the distant wave zone, $x \equiv \omega r/c \gg 1$,

$$n_2(x) - i\epsilon j_2(x) = \frac{e^{i\epsilon x}}{x} ; \tag{16.83}$$

in the near zone $x = \omega r/x \ll 1$,

$$n_2(x) = -\frac{3}{x^3}\left(1 \;\&\; x^2 \;\&\; x^4 \;\&\; \ldots\right) , \quad j_2(x) = \frac{x^2}{15}\left(1 \;\&\; x^2 \;\&\; x^4 \;\&\; \ldots\right) . \tag{16.84}$$

Here "& x^n" means "+ (some constant)x^n".

****

16.6 T2 Convection

In this last section of Chap 15, we turn attention to fluid motions driven by thermal effects (see the overview in Sec. 16.1). As a foundation, we begin by discussing heat transport via thermal diffusion:

16.6.1 T2 Heat Conduction

We know experimentally that heat flows in response to a temperature gradient. When the temperature differences are small on the scale of the mean free path of the heat-conducting particles (as, in practice, almost always will be the case), then we can expand the heat flux as a Taylor series in the temperature gradient, $\mathbf{F}_{\rm heat}$ = (constant) + (a term linear in $\boldsymbol{\nabla} T$) + (a term quadratic in $\boldsymbol{\nabla} T$) + ... Now, the constant term must vanish; otherwise there would be heat conduction in the absence of a temperature gradient and this would contradict the second law of thermodynamics. The first contributing term is thus the linear term, and we stop with it, just as we do for Hooke's law of elasticity and Ohm's law of electrical conductivity. Here, as in elasticity and electromagnetism, we must be on the lookout for special circumstances when the linear approximation becomes invalid and be prepared to modify our description accordingly. This rarely happens in fluid dynamics, so in this chapter we shall ignore higher-order terms and write

$$\boxed{\mathbf{F}_{\rm heat} = -\kappa \boldsymbol{\nabla} T ,} \tag{16.85}$$

where the constant κ is known as the *coefficient of thermal conductivity* or just the thermal conductivity; cf. Secs. 2.7 and 12.7.3, where we have discussed it previously. In general κ will

be a tensor, as it describes a linear relation between two vectors $\mathbf{F}_{\rm heat}$ and $\boldsymbol{\nabla} T$. However, when the fluid is isotropic (as it is for the kinds of fluids we have treated thus far), κ is just a scalar. We shall confine ourselves to this case in the present chapter; but in Chap. 18, when describing a plasma as a fluid, we shall find that a magnetic field can make the plasma's transport properties be decidedly anisotropic, so the thermal conductivity is tensorial.

In this section we shall discuss how heat conduction is incorporated into the fundamental equations of fluid dynamics—focusing on the underlying physics and on approximations, by contrast with our earlier quite formal analysis in Sec. 12.7.3.

Heat conduction can be incorporated most readily via the conservation laws for momentum and energy. On the molecular scale, the diffusing heat shows up as an anisotropic term $\mathcal{N}_1$ in the momentum distributions $\mathcal{N}(\mathbf{p}) = \mathcal{N}_0 + \mathcal{N}_1$ of particles (molecules, atoms, electrons, photons, ...); cf., e.g., Eqs. (2.74a) and (2.74g). This anisotropic term is tiny in magnitude compared to the isotropic term $\mathcal{N}_0$, which has already been included via $u =$(internal energy per unit mass) and $P =$ (pressure) in our densities and fluxes of momentum and energy. The only place that the molecular-scale anisotropic term is of any quantitative consequence, macroscopically, is in the energy flux; so heat conductivity modifies only the energy flux and not the energy density or the momentum density or flux.[5] Correspondingly, the law of momentum conservation (the Navier-Stokes equation) is left unchanged, while energy conservation is altered.

We explored the modifications of energy conservation, formally, in Sec. 12.7.3. As we discussed there, energy conservation is most powerfully expressed in the language of entropy. For an inviscid fluid with vanishing heat conductivity, energy conservation is equivalent to the constancy of the the entropy per unit mass s moving with the fluid, $ds/dt = 0$. When viscosity and heat conductivity are turned on, then the entropy changes moving with a fluid element in the following manner:

$$\boxed{\rho T \frac{ds}{dt} = \kappa \nabla^2 T + 2\eta \boldsymbol{\sigma} : \boldsymbol{\sigma} + \zeta \theta^2 \ .} \tag{16.86}$$

[This version of entropy evolution is deduced in Ex. 16.16 from one of the versions we wrote down in Chap. 12, Eq. (12.71).]

This equation is most easily understood, physically, by rewriting it as $\rho T ds/dt + \boldsymbol{\nabla} \cdot (-\kappa \boldsymbol{\nabla} T) = +2\eta \boldsymbol{\sigma} : \boldsymbol{\sigma} + \zeta \theta^2$. The left side is the rate of change of the thermal energy density in the rest frame of the fluid (a time derivative of the thermal energy density, since Tds is the rate dQ at which heat is injected into a unit mass, plus the divergence of the thermally diffusing energy flux). Thye right side is the rate of viscous heating per unit volume.

For a viscous, heat-conducting fluid moving in an external gravitational field, the governing equations are the standard law of mass conservation (12.25) or (12.27), the standard Navier-Stokes equation (12.65), the first law of thermodynamics [Eq. (2) or (3) of Box 12.2], and the law of entropy evolution (16.86).

This set of equations is far too complicated to solve, except via massive numerical simulations, unless some strong simplification is imposed. We must therefore introduce approxima-

[5] This is only true non-relativistically. In relativistic fluid dynamics, it remains true in the fluid's rest frame; but in frames where the fluid moves at high speed, the diffusive energy flux gets Lorentz transformed into heat-flow contributions to energy density, momentum density, and momentum flux.

tions. *Our first approximation* (already implicit in the above equations) *is that the thermal conductivity κ is constant;* for most real applications this is close to true, and no significant physical effects are missed by assuming it. *Our second approximation,* which does limit somewhat the type of problem we can address, is that *the fluid motions are very slow*—slow enough that the squares of the shear and expansion (which are quadratic in the fluid speed) are neglibibly small, and we thus can ignore viscous dissipation. This permits us to rewrite the entropy evolution equation (16.86) as the law of energy conservation in the fluid's rest frame

$$\rho T \frac{ds}{dt} = \kappa \nabla^2 T. \tag{16.87}$$

We can convert this entropy evolution equation into an evolution equation for temperature by expressing the changes ds/dt of entropy per baryon in terms of changes dT/dt of temperature. The usual way to do this is to note that Tds (the amount of heat deposited in a unit mass of fluid) is given by CdT, where C is the fluid's specific heat. However, the specific heat depends on what one holds fixed during the energy deposition: the fluid element's volume or its pressure. As we have assumed that the fluid motions are very slow, the fractional pressure fluctuations will be correspondingly small. (This does not preclude significant temperature fluctuations, provided that they are compensated by density fluctuations of opposite sign. However, if there are temperature fluctuations, then these will tend to equalize through thermal conduction in such a way that the pressure does not change significantly.) Therefore, the relevant specific heat for a slowly moving fluid is the one at constant pressure, C_P, and we must write $Tds = C_P dT$.[6] Eq. (16.87) then becomes a linear partial differential equation for the temperature

$$\boxed{\frac{dT}{dt} \equiv \frac{\partial T}{\partial t} + \mathbf{v} \cdot \boldsymbol{\nabla} T = \chi \nabla^2 T \ ,} \tag{16.88}$$

where

$$\boxed{\chi = \kappa / \rho C_p} \tag{16.89}$$

is known as the *thermal diffusivity* and we have again taken the easiest route in treating C_P and ρ as constant. When the fluid moves so slowly that the advective term $\mathbf{v} \cdot \boldsymbol{\nabla} T$ is negligible, then Eq. (16.88) says that the heat simply diffuses through the fluid, with the thermal diffusivity being the diffusion coefficient for the temperature.

The diffusive transport of heat by thermal conduction is similar to the diffusive transport of vorticity by viscous stress [Eq. (13.3)] and the thermal diffusivity χ is the direct analog of the kinematic viscosity ν. This motivates us to introduce a new dimensionless number known as the *Prandtl number*, which measures the relative importance of viscosity and heat conduction (in the sense of their relative abilities to produce a diffusion of vorticity and of heat):

$$\boxed{\mathrm{Pr} = \frac{\nu}{\chi}} \tag{16.90}$$

[6] See e.g. Turner 1973 for a more formal justification of the use of the specific heat at constant pressure rather than constant volume.

For gases, both ν and χ are given to order of magnitude by the product of the mean molecular speed and the mean free path and so Prandtl numbers are typically of order unity. (For air, Pr $\sim$ 0.7.) By contrast, in liquid metals the free electrons carry heat very efficiently compared with the transport of momentum (and vorticity) by diffusing ions, and so their Prandtl numbers are small. This is why liquid sodium is used as a coolant in nuclear power reactors. At the other end of the spectrum, water is a relatively poor thermal conductor with Pr $\sim$ 6, and Prandtl numbers for oils, which are quite viscous and poor conductors, measure in the thousands. Other Prandtl numbers are given in Table 16.1.

Fluid	ν (m^2s^{-1})	χ (m^2s^{-1})	Pr
Earth's mantle	10^{17}	10^{-6}	10^{23}
Solar interior	10^{-2}	10^{2}	10^{-4}
Atmosphere	10^{-5}	10^{-5}	1
Ocean	10^{-6}	10^{-7}	10

Table 16.1: Order of magnitude estimates for kinematic viscosity ν, thermal diffusivity χ, and Prandtl number Pr $= \nu/\chi$ for earth, fire, air and water.

One might think that, when the Prandtl number is small (so κ is large compared to ν), one should necessarily include heat flow in the fluid equations. Not so. One must distinguish the flow from the fluid. In some low-Prandtl-number flows, the heat conduction is so effective that the fluid becomes essentially isothermal, and buoyancy effects are minimised. Conversely, in some large-Prandtl-number flows the large viscous stress reduces the velocity gradient so that slow, thermally driven circulation takes place and thermal effects are very important. In general, the kinematic viscosity is of direct importance in controlling the transport of momentum, and hence in establishing the velocity field, whereas heat conduction enters only indirectly (Sec. 16.6.2 below). We must therefore examine each flow on its individual merits.

There is another dimensionless number that is commonly introduced when discussing thermal effects: the *Péclet number*. It is defined, by analogy with the Reynolds' number, by

$$\boxed{\mathrm{Pe} = \frac{VL}{\chi}} \ , \tag{16.91}$$

where L is a characteristic length scale of the flow and V is a characteristic speed. The Péclet number measures the relative importance of advection and heat conduction.

****

EXERCISES

Exercise 16.16 *Derivation: Equations for Entropy Evolution*
By combining the law of energy increase (12.71) (which is equivalent to energy conservation) with the law of mass conservation, derive Eq. (16.86) for the evolution of the fluid's entropy.

Exercise 16.17 *Example: Poiseuille Flow with a uniform temperature gradient*
A nuclear reactor is cooled with liquid sodium which flows through a set of pipes from the reactor to a remote heat exchanger, where the heat's energy is used to generate electricity. Unfortunately, some heat will be lost through the walls of the pipe before it reaches the heat exchanger and this will reduce the reactor's efficiency. In this question, we determine what fraction of the heat is lost through the pipe walls.

Consider the flow of the sodium through one of the pipes, and assume that the Reynold's number is modest so the flow is steady and laminar. Then the fluid velocity will have the parabolic Poiseuille profile

$$v = 2\bar{v}\left(1 - \frac{\varpi^2}{R^2}\right) \tag{16.92}$$

[Eq. (12.76) and associated discussion]. Here R is the pipe's inner radius, ϖ is the cylindrical radial coordinate measured from the axis of the pipe, and $\bar{v}$ is the mean speed along the pipe. Suppose that the pipe has length $L \gg R$ from the reactor to the heat exchanger, and is thermally very well insulated so its inner wall is at nearly the same temperature as the core of the fluid. Then the total temperature drop ΔT down the length L will be $\Delta T \ll T$, and the temperature gradient will be constant, so the temperature distribution in the pipe has the form

$$T = T_0 - \Delta T\frac{z}{L} + f(\varpi)\ . \tag{16.93}$$

(a) Use Eq. (16.87) to show that

$$f = \frac{\bar{v}R^2\Delta T}{2\chi L}\left[\frac{3}{4} - \frac{\varpi^2}{R^2} + \frac{1}{4}\frac{\varpi^4}{R^4}\right]\ . \tag{16.94}$$

(b) Derive an expression for the conductive heat flux through the walls of the pipe and show that the ratio of the heat escaping through the walls to that convected by the fluid is $\Delta T/T$. (Ignore the influence of the temperature gradient on the velocity field and treat the thermal diffusivity and specific heat as constant throughout the flow.)

(c) Consider a nuclear reactor in which 10kW of power has to be transported through a pipe carrying liquid sodium. If the reactor temperature is $\sim$ 1000K and the exterior temperature is room temperature, estimate the flow of liquid sodium necessary to achieve the necessary transport of heat

.

Exercise 16.18 *Problem: Thermal Boundary Layers*
In Sec. 13.4, we introduced the notion of a laminar boundary layer by analyzing flow past a thin plate. Now suppose that this same plate is maintained at a different temperature from the free flow. A thermal boundary layer will be formed, in addition to the viscous boundary layer, which we presume to be laminar. These two boundary layers will both extend outward from the wall but will (usually) have different thicknesses.

(a) Explain why their relative thicknesses depend on the Prandtl number.

(b) Using Eq. (16.88), show that in order of magnitude the thickness of the thermal boundary layer, δ_T, is given by

$$v(\delta_T)\delta_T^2 = \ell\chi \ ,$$

where $v(\delta_T)$ is the fluid velocity parallel to the plate at the outer edge of the thermal boundary layer and ℓ is the distance downstream from the leading edge. Let V be the free stream fluid velocity and ΔT be the temperature difference between the plate and the body of the flow.

(c) Estimate δ_T in the limits of large and small Prandtl numbers.

(d) What will be the boundary layer's temperature profile when the Prandtl number is exactly unity?

****

16.6.2 T2 Boussinesq Approximation

When the heat fluxes are sufficiently small, we can use Eq. (16.88) to solve for the temperature distribution in a given velocity field, ignoring the feedback of the thermal effects onto the velocity. However, if we imagine increasing the flow's temperature differences so the heat fluxes also increase, at some point thermal feedback effects will begin to influence the velocity significantly. The first feedback effect to occur is typically that of *buoyancy*, the tendency of the hotter (and hence lower-density) fluid to rise in a gravitational field and the colder (and hence denser) fluid to descend.[7] In this section, we shall describe the effects of buoyancy as simply as possible. The minimal approach, which is adequate surprisingly often, is called the *Boussinesq approximation*. It can be used to describe many laboratory flows and atmospheric flows, and some geophysical flows.

The type of flows for which the Boussinesq approximation is appropriate are those in which the fractional density changes are small ($|\Delta\rho| \ll \rho$). By contrast, the velocity can undergo large changes. However, as the density changes following a fluid element must be small, $\rho^{-1}d\rho/dt \simeq 0$, we can approximate the equation of continuity (mass conservation) $d\rho/dt + \rho\boldsymbol{\nabla}\cdot\mathbf{v} = 0$ by the "incompressibility" relation

$$\boxed{\boldsymbol{\nabla}\cdot\mathbf{v} = 0 \ . \quad \text{Boussinesq (1)}} \tag{16.95}$$

This does not mean that the density is constant. Rather, it means that the sole significant cause of density changes is thermal expansion. In discussing thermal expansion, it is convenient to introduce a reference density ρ_0 and reference temperature T_0, equal to some mean of the density and temperature in the region of fluid that one is studying. We shall denote by

$$\boxed{\tau \equiv T - T_0} \tag{16.96}$$

[7] This effect is put to good use in a domestic "gravity-fed" warm-air circulation system. The furnace generally resides in the basement not the attic!

the perturbation of the temperature away from its reference value. The thermally perturbed density can then be written as

$$\boxed{\rho = \rho_0(1 - \alpha\tau) \ ,} \tag{16.97}$$

where α is the thermal expansion coefficient for volume[8] [evaluated at constant pressure for the same reason as C_P was at constant pressure in the paragraph following Eq. (16.87)]:

$$\boxed{\alpha = -\left(\frac{\partial \ln \rho}{\partial T}\right)_P \ .} \tag{16.98}$$

Equation (16.97) enables us to eliminate density perturbations as an explicit variable and replace them by temperature perturbations.

Turn, now, to the Navier-Stokes equation (12.66) in a uniform external gravitational field:

$$\frac{d\mathbf{v}}{dt} = -\frac{\boldsymbol{\nabla} P}{\rho} + \boldsymbol{g} + \nu\nabla^2\mathbf{v} \ . \tag{16.99}$$

We expand the pressure-gradient term as

$$-\frac{\boldsymbol{\nabla} P}{\rho} \simeq -\frac{\boldsymbol{\nabla} P}{\rho_0}(1 + \alpha\tau) \ , \tag{16.100}$$

and, as in our analysis of rotating flows [Eq. (13.53)], we introduce an *effective pressure* designed to compensate for the first-order effects of the uniform gravitational field:

$$\boxed{P' = P + \rho_0\Phi = P - \rho_0 \boldsymbol{g}\cdot\mathbf{x} \ .} \tag{16.101}$$

(Notice that P' measures the amount the pressure differs from the value it would have in supporting a hydrostatic atmosphere of the fluid at the reference density.) The Navier-Stokes equation (16.99) then becomes

$$\boxed{\frac{d\mathbf{v}}{dt} = -\frac{\boldsymbol{\nabla} P'}{\rho_0} - \alpha\tau\boldsymbol{g} + \nu\nabla^2\mathbf{v} \ , \quad \text{Boussinesq (2)}} \tag{16.102}$$

dropping the small term $O(\alpha P')$. In words, a fluid element accelerates in response to a buoyancy force which is the sum of the first and second terms on the right hand side of Eq. (16.102), and a viscous force.

In order to solve this equation we must be able to solve for the temperature perturbation, τ. This evolves according to the standard equation of heat diffusion, Eq. (16.88):

$$\boxed{\frac{d\tau}{dt} = \chi\nabla^2\tau. \quad \text{Boussinesq (3)}} \tag{16.103}$$

Equations (16.95), (16.102) and (16.103) are the equations of fluid flow in the Boussinesq approximation; they control the coupled evolution for the velocity $\mathbf{v}$ and the temperature perturbation τ. We shall now use them to discuss free convection in a laboratory apparatus.

[8]Note that α is three times larger than the thermal expansion coefficient for the linear dimensions of the fluid.

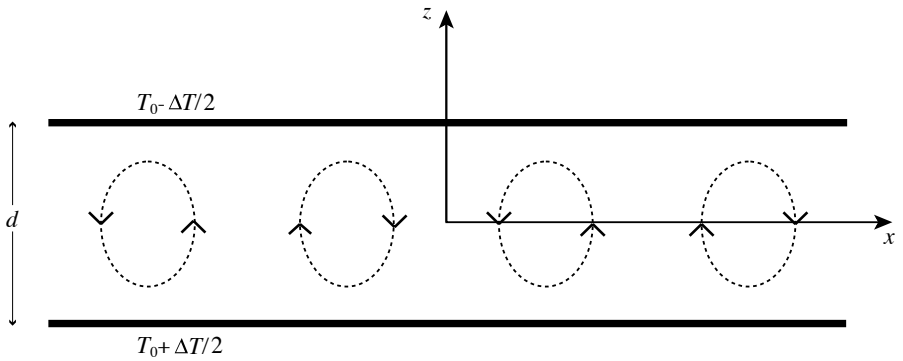

Fig. 16.11: Rayleigh-Bénard convection. A fluid is confined between two horizontal surfaces separated by a vertical distance d. When the temperature difference between the two plates ΔT is increased sufficiently, the fluid will start to convect heat vertically. The reference effective pressure P'_0 and reference temperature T_0 are the values of P' and T measured at the midplane $z = 0$.

16.6.3 T2 Rayleigh-Bénard Convection

In a relatively simple laboratory experiment to demonstrate convection, a fluid is confined between two rigid plates a distance d apart, each maintained at a fixed temperature, with the upper plate cooler than the lower by ΔT. When ΔT is small, viscous stresses, together with the no-slip boundary conditions at the plates, inhibit circulation; so, despite the upward boyancy force on the hotter, less-dense fluid near the bottom plate, the fluid remains stably at rest with heat being conducted diffusively upward. If the plates' temperature difference ΔT is gradually increased, the buoyancy becomes gradually stronger. At some critical ΔT it will overcome the restraining viscous forces, and the fluid will start to circulate (convect) between the two plates. Our goal is to determine the critical temperature difference $\Delta T_{\rm crit}$ for the onset of convection.

We now make some physical arguments to simplify the calculation of $\Delta T_{\rm crit}$. From our experience with earlier instability calculations, especially those involving elastic bifurcations (Secs. 10.8 and 11.3.5), we anticipate that for $\Delta T < \Delta T_{\rm crit}$ the response of the equilibrium to small perturbations will be oscillatory (i.e., will have positive squared eigenfrequency ω^2), while for $\Delta T > \Delta T_{\rm crit}$, perturbations will grow exponentially (i.e., will have negative ω^2). Correspondingly, at $\Delta T = \Delta T_{\rm crit}$, ω^2 for some mode will be zero. This zero-frequency mode will mark the bifurcation of equilibria from one with no fluid motions to one with slow, convective motions. We shall search for $\Delta T_{\rm crit}$ by searching for a solution to the Boussinesq equations (16.95), (16.102) and (16.103) that represents this zero-frequency mode. In those equations we shall choose for the reference temperature T_0, density ρ_0 and effective pressure P_0 the values at the midplane between the plates, $z = 0$; cf. Fig. 16.11.

The unperturbed equilibrium, when $\Delta T = \Delta T_{\rm crit}$, is a solution of the Boussinesq equations (16.95), (16.102) and (16.103) with vanishing velocity, a time-independent vertical temperature gradient $dT/dz = -\Delta T/d$, and a compensating, time-independent, vertical pressure gradient:

$$\mathbf{v} = 0 \ , \quad \tau = T - T_0 = -\frac{\Delta T}{d} z \ , \quad P' = P'_0 + g\rho_0\alpha \frac{\Delta T}{d}\frac{z^2}{2} \ . \tag{16.104}$$

When the zero-frequency mode is present, the velocity $\mathbf{v}$ will be nonzero, and the temperature and effective pressure will have additional perturbations $\delta\tau$ and $\delta P'$:

$$\mathbf{v} \neq 0 \ , \quad \tau = T - T_0 = -\frac{\Delta T}{d} z + \delta\tau \ , \quad P' = P'_0 + g\rho_0\alpha\frac{\Delta T}{d}\frac{z^2}{2} + \delta P' \ . \tag{16.105}$$

The perturbations $\mathbf{v}$, $\delta\tau$ and $\delta P'$ are governed by the Boussinesq equations and the boundary conditions $\mathbf{v} = 0$ (no-slip) and $\delta\tau = 0$ at the plates, $z = \pm d/2$. We shall manipulate these in such a way as to get a partial differential equation for the scalar temperature perturbation $\delta\tau$ by itself, decoupled from the velocity and the pressure perturbation.

Consider, first, the result of inserting expressions (16.105) into the Boussinesq-approximated Navier-Stokes equation (16.102). Because the perturbation mode has zero frequency, $\partial v/\partial t$ vanishes; and because $\mathbf{v}$ is extremely small, we can neglect the quadratic advective term $\mathbf{v}\cdot\nabla\mathbf{v}$, thereby bringing Eq. (16.102) into the form

$$\frac{\boldsymbol{\nabla}\delta P'}{\rho_0} = \nu\nabla^2\mathbf{v} - \boldsymbol{g}\alpha\delta\tau \ . \tag{16.106}$$

We want to eliminate $\delta P'$ from this equation. The other Boussinesq equations are of no help for this, since $\delta P'$ is absent from them. When we dealt with sound waves, we eliminated δP using the equation of state $P = P(\rho, T)$; but in the present analysis our Boussinesq approximation insists that the only significant changes of density are those due to thermal expansion, i.e. it neglects the influence of pressure on density, so the equation of state cannot help us. Lacking any other way to eliminate $\delta P'$, we employ a very common trick: we take the curl of Eq. (16.106). As the curl of a gradient vanishes, $\delta P'$ drops out. We then take the curl one more time and use the fact that $\boldsymbol{\nabla}\cdot\mathbf{v} = 0$ to obtain

$$\nu\nabla^2(\nabla^2\mathbf{v}) = \alpha\boldsymbol{g}\nabla^2\delta\tau - \alpha(\boldsymbol{g}\cdot\nabla)\nabla\delta\tau \ . \tag{16.107}$$

Turn, next, to the Boussinesq version of the equation of heat transport, Eq. (16.103). Inserting into it Eqs. (16.105) for τ and $\mathbf{v}$, setting $\partial\delta\tau/\partial t$ to zero because our perturbation has zero frequency, linearizing in the perturbation, and using $\boldsymbol{g} = -g\mathbf{e}_z$, we obtain

$$\frac{v_z\Delta T}{d} = -\chi\nabla^2\delta\tau \ . \tag{16.108}$$

This is an equation for the vertical velocity v_z in terms of the temperature perturbation $\delta\tau$. By inserting this v_z into the z component of Eq. (16.107), we achieve our goal of a scalar equation for $\delta\tau$ alone:

$$\boxed{\nu\chi\nabla^2\nabla^2\nabla^2\delta\tau = \frac{\alpha g\Delta T}{d}\left(\frac{\partial^2\delta\tau}{\partial x^2} + \frac{\partial^2\delta\tau}{\partial y^2}\right) \ .} \tag{16.109}$$

This is a sixth order differential equation, even more formidable than the fourth order equations that arise in the elasticity calculations of Chaps. 10 and 11. We now see how prudent it was to make simplifying assumptions at the outset!

The differential equation (16.109) is, however, linear, and we can seek solutions using separation of variables. As the equilibrium is unbounded horizontally, we look for a single horizontal Fourier component with some wave number k; i.e., we seek a solution of the form

$$\delta\tau \propto \exp(ikx) f(z) \ , \tag{16.110}$$

where $f(z)$ is some unknown function. Such a $\delta\tau$ will be accompanied by motions $\mathbf{v}$ in the x and z directions (i.e., $v_y = 0$) that also have the form $v_j \propto \exp(ikx) f_j(z)$ for some other functions $f_j(z)$.

The anszatz (16.110) converts the partial differential equation (16.109) into the single ordinary differential equation

$$\left(\frac{d^2}{dz^2} - k^2\right)^3 f + \frac{\mathrm{Ra}\, k^2 f}{d^4} = 0 \ , \tag{16.111}$$

where we have introduced yet another dimensionless number

$$\boxed{\mathrm{Ra} = \frac{\alpha g \Delta T d^3}{\nu\chi}} \tag{16.112}$$

called the *Rayleigh number*. By virtue of the relation (16.108) between v_z and $\delta\tau$, the Rayleigh number is a measure of the ratio of the strength of the buoyancy term $-\alpha\delta\tau\boldsymbol{g}$ to the viscous term $\nu\nabla^2\mathbf{v}$ in the Boussinesq version (16.102) of the Navier-Stokes equation:

$$\boxed{\mathrm{Ra} \sim \frac{\text{buoyancy force}}{\text{viscous force}} \ .} \tag{16.113}$$

The general solution of Eq. (16.111) is an arbitrary, linear combination of three sine functions and three cosine functions:

$$f = \sum_{n=1}^{3} A_n \cos(\mu_n k z) + B_n \sin(\mu_n k z) \ , \tag{16.114}$$

where the dimensionless numbers μ_n are given by

$$\mu_n = \left[\left(\frac{\mathrm{Ra}}{k^4 d^4}\right)^{1/3} e^{2\pi n i/3} - 1\right]^{1/2} \ ; \quad n = 1, 2, 3 \ , \tag{16.115}$$

which involves the three cube roots of unity, $e^{2\pi n i/3}$. The values of five of the coefficients A_n, B_n are fixed in terms of the sixth (an overall arbitrary amplitude) by five boundary conditions at the bounding plates, and a sixth boundary condition then determines the critical temperature difference ΔT_{crit} (or equivalently, the critical Rayleigh number $\mathrm{Ra}_{\mathrm{crit}}$) at which convection sets in.

The six boundary conditions are: (i) The requirement that the fluid temperature be the same as the plate temperature at each plate, so $\delta\tau = 0$ at $z = \pm d/2$. (ii) The no-slip boundary condition $v_z = 0$ at each plate which, by virtue of Eq. (16.108) and $\delta\tau = 0$

at the plates, translates into $\delta\tau_{,zz} = 0$ at $z = \pm d/2$ (where the indices after the comma are partial derivatives). (iii) The no-slip boundary condition $v_x = 0$, which by virtue of incompressibility $\boldsymbol{\nabla}\cdot\mathbf{v} = 0$ implies $v_{z,z} = 0$ at the plates, which in turn by Eq. (16.108) implies $\delta\tau_{,zzz} + \delta\tau_{,xxz} = 0$ at $z = \pm d/2$.

It is straightforward but computationally complex to impose these six boundary conditions and from them deduce the critical Rayleigh number for onset of convection; see Pellew and Southwell (1940). Rather than present the nasty details, we shall switch to a toy problem in which the boundary conditions are adjusted to give a simpler solution, but one with the same qualitative features as for the real problem. Specifically, we shall replace the no-slip condition (iii) ($v_x = 0$ at the plates) by a condition of no shear, (iii') $v_{x,z} = 0$ at the plates. By virtue of incompressibility $\boldsymbol{\nabla}\cdot\mathbf{v} = 0$, the x derivative of this translates into $v_{z,zz} = 0$, which by Eq. (16.108) translates to $\delta\tau_{,zzxx} + \delta\tau_{,zzzz} = 0$. To recapitulate, we seek a solution of the form (16.114), (16.115) that satisfies the boundary conditions (i), (ii), (iii').

The terms in Eq. (16.114) with $n = 1, 2$ always have complex arguments and thus always have z dependences that are products of hyperbolic and trigonometric functions with real arguments. For $n = 3$ and large enough Rayleigh number, μ_3 is positive and the solutions are pure sines and cosines. Let us just consider the $n = 3$ terms alone, in this regime, and impose boundary condition (i), that $\delta\tau = 0$ at the plates. The cosine term by itself,

$$\delta\tau = \text{constant} \times \cos(\mu_3 kz)\, e^{ikx} \ , \tag{16.116}$$

satisfies this, if we set

$$\frac{\mu_3 kd}{2} \equiv \left[\left(\frac{\mathrm{Ra}}{k^4 d^4}\right)^{1/3} - 1\right]^{1/2} \frac{kd}{2} = (m + 1/2)\pi \ , \tag{16.117}$$

where m is an integer. It is straightforward to show, remarkably, that Eqs. (16.116), (16.117) also satisfy boundary conditions (ii) and (iii'), so they solve the toy version of our problem.

As ΔT is gradually increased from zero, the Rayleigh number Ra gradually grows, passing one after another through the sequence of values (16.117) with $m = 0, 1, 2, ...$ (for any chosen k). At each of these values there is a zero-frequency, circulatory mode of fluid motion with horizontal wave number k, which is passing from stability to instability. The first of these, $m = 0$, represents the onset of circulation for the chosen k, and the Rayleigh number at this onset [Eq. (16.117) with $m = 0$] is

$$\mathrm{Ra} = \frac{(k^2 d^2 + \pi^2)^3}{k^2 d^2} \ . \tag{16.118}$$

This $\mathrm{Ra}(k)$ relation is plotted as a thick curve in Fig. 16.12.

Notice in Fig. 16.12 that there is a critical Rayleigh number $\mathrm{Ra}_{\mathrm{crit}}$ below which all modes are stable, independent of their wave numbers, and above which modes in some range $k_{\min} < k < k_{\max}$ are unstable. From Eq. (16.118) we deduce that, for our toy problem, $\mathrm{Ra}_{\mathrm{crit}} = 27\pi^4/4 \simeq 660$.

When one imposes the correct boundary conditions (i), (ii), (iii) [instead of our toy choice (i), (ii), (iii')] and works through the nasty details of the computation, one obtains a $\mathrm{Ra}(k)$

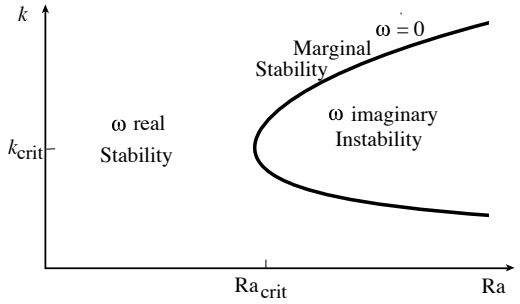

Fig. 16.12: Horizontal wave number k of the first mode to go unstable, as a function of Rayleigh number, Ra. Along the solid curve the mode has zero frequency; to the left of the curve it is stable, to the right it is unstable. $Ra_{\rm crit}$ is the minimum Rayleigh number for convective instability.

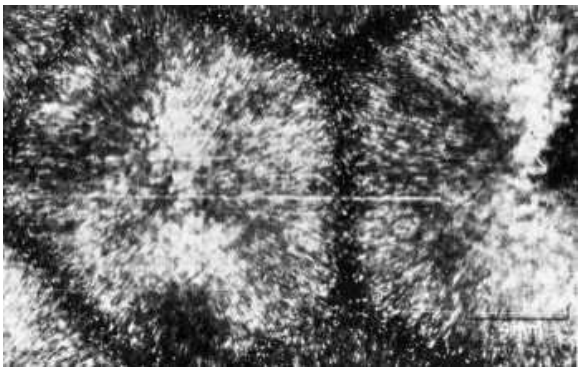

Fig. 16.13: Hexagonal convection cells in Rayleigh-Bénard convection. The fluid, which is visualized using aluminum powder, rises at the centers of the hexagons and falls around the edges.

relation that looks qualitatively the same as Fig. 16.12, one deduces that convection should set in at $\mathrm{Ra}_{\rm crit} \simeq 1700$, which agrees reasonably well with experiment. One can carry out the same computation with the fluid's upper surface free to move (e.g., due to placing air rather than a solid plate at $z = d/2$). Such a computation predicts that convection begins at $\mathrm{Ra}_{\rm crit} \simeq 1100$, though in practice surface tension is usually important and its effect must be included.

One feature of these critical Rayleigh numbers is very striking. Because the Rayleigh number is an estimate of the ratio of buoyancy forces to viscous forces [Eq. (16.113)], an order-of-magnitude analysis suggests that convection should set in at $\mathrm{Ra} \sim 1$—which is wrong by three orders of magnitude! This provides a vivid reminder that order-of-magnitude estimates can be quite inaccurate. In this case, the main reason for the discrepancy is that the convective onset is governed by a sixth-order differential equation (16.109), and thus is very sensitive to the lengthscale d used in the order-of-magnitude analysis. If we choose d/π rather than d as the length scale, then an order-of-magnitude estimate could give $\mathrm{Ra} \sim \pi^6 \sim 1000$, a much more satisfactory value.

Once convection has set in, the unstable modes grow until viscosity and nonlinearities stabilize them, at which point they carry far more heat upward between the plates than does conduction. The convection's velocity pattern depends, in practice, on the manner in which

the heat is applied and the temperature dependence of the viscosity. For a limited range of Rayleigh numbers near $\mathrm{Ra}_{\mathrm{crit}}$, it is possible to excite a hexagonal pattern of *convection cells* as shown in Fig. 16.13. When the Rayleigh number becomes very large, the convection becomes fully turbulent and we must introduce an effective turbulent viscosity to replace the molecular viscosity (cf. Chap. 14).

Free convection, like that in this laboratory experiment, also occurs in meteorological and geophysical flows. For example for air in a room, the relevant parameter values are $\alpha = 1/T \sim 0.003\ \mathrm{K}^{-1}$ (Charles' Law), and $\nu \sim \chi \sim 10^{-5}\ \mathrm{m}^2\ \mathrm{s}^{-1}$, so the Rayleigh number is $\mathrm{Ra} \sim 3\times 10^8 (\Delta T/1\mathrm{K})(d/1\mathrm{m})^3$. Convection in a room thus occurs extremely readily, even for small temperature differences. In fact, so many modes of convective motion can be excited that heat-driven air flow is invariably turbulent. It is therefore common in everyday situations to describe heat transport using a phenomenological turbulent thermal conductivity (cf. section 14.3). A further example is given in Box 16.3.

****

EXERCISES

Exercise 16.19 *Problem: Critical Rayleigh Number*
Estimate the temperature to which pans of oil ($\nu \sim 10^{-5}\ \mathrm{m}^2\ \mathrm{s}^{-1}$, Pr$\sim$ 3000), water ($\nu \sim 10^{-6}\ \mathrm{m}^2\ \mathrm{s}^{-1}$, Pr$\sim$ 6) and mercury ($\nu \sim 10^{-7}\ \mathrm{m}^2\ \mathrm{s}^{-1}$, Pr$\sim$ 0.02) would have to be heated in order to convect. Assume that the upper surface is at room temperature. Do not perform this experiment with mercury!

Exercise 16.20 *Problem: Width of Thermal Plume*
Consider a two dimensional thermal plume transporting heat away from a hot knife edge. Introduce a temperature deficit $\Delta T(z)$ measuring the typical difference in temperature between the plume and the surrounding fluid at height z above the knife edge, and let $\delta_p(z)$ be the width of the plume at height z.

(a) Show that energy conservation implies the constancy of $\delta_p \Delta T \bar{v}_z$, where $\bar{v}_z(z)$ is the plume's mean vertical speed at height z.

(b) Make an estimate of the buoyancy acceleration and use this to estimate $\bar{v}_z$.

(c) Use Eq. (16.103) to relate the width of the plume to the speed. Hence, show that the width of the plume scales as $\delta_p \propto z^{2/5}$ and the temperature deficit as $\Delta T \propto z^{-3/5}$.

(d) Repeat this exercise for a three dimensional plume above a hot spot.

****

Box 16.3
Mantle Convection and Continental Drift

As is now well known, the continents drift over the surface of the globe on a timescale of roughly a hundred million years. Despite the clear geographical evidence that the continents fit together, geophysicists were, for a long while, skeptical that this occured because they were unable to identify the forces responsible for overcoming the visco-elastic resilience of the crust. It is now known that these motions are in fact slow convective circulation of the mantle driven by internally generated heat from the radioactive decay of unstable isotopes, principally uranium, thorium and potassium.

When the heat is generated within the convective layer, rather than passively transported from below, we must modify our definition of the Rayleigh number. Let the heat generated per unit mass per unit time be Q. In the analog of our laboratory analysis, where the fluid is assumed marginally unstable to convective motions, this Q will generate a heat flux $\sim \rho Q d$, which must be carried diffusively. Equating this flux to $\kappa \Delta T/d$, we can solve for the temperature difference ΔT between the lower and upper edges of the convective mantle: $\Delta T \sim \rho Q d^2/\kappa$. Inserting this ΔT into Eq. (16.112), we obtain a modified expression for the Rayleigh number

$$\mathrm{Ra}' = \frac{\alpha \rho g Q d^5}{\kappa \chi \nu} \ . \tag{1}$$

Let us now estimate the value of Ra' for the earth's mantle. The mantle's kinematic viscosity can be measured by post-glacial rebound studies (cf. Ex. 13.5) to be $\sim 10^{17}$ $\mathrm{m^2\ s^{-1}}$. We can use the rate of attenuation of diurnal and annual temperature variation with depth in surface rock to estimate a thermal diffusivity $\chi \sim 10^{-6}$ $\mathrm{m^2\ s^{-1}}$. Direct experiment furnishes an expansion coefficient, $\alpha \sim 3 \times 10^{-5}$ $\mathrm{K^{-1}}$. The thickness of the upper mantle is roughly 700 km and the rock density is about 4000 kg $\mathrm{m^{-3}}$. The rate of heat generation can be estimated both by chemical analysis and direct measurement at the earth's surface and turns out to be $Q \sim 10^{-11}$ W $\mathrm{kg^{-1}}$. Combining these quantities, we obtain an estimated Rayleigh number $\mathrm{Ra}' \sim 10^6$, well in excess of the critical value for convection under free slip conditions which evaluates to 868 (Turcotte & Schubert 1982). For this reason, it is now believed that continental drift is driven primarily by mantle convection.

16.6.4 T2 Convection in Stars

The sun and other stars generate heat in their interiors by nuclear reactions. In most stars, the internal energy is predominantly in the form of hot hydrogen and helium ions and their electrons, while the thermal conductivity is due primarily to diffusing photons (Sec. 2.7), which have much longer mean free paths than the ions and electrons. When the photon mean free path becomes small due to high opacity (as happens in the outer 30 per cent of the sun; Fig. 16.14), the thermal conductivity goes down, so in order to transport the heat from nuclear burning, the star develops an increasingly steep temperature gradient. The

star may then become convectively unstable and transport its energy far more efficiently by circulating its hot gas than it could have by photon diffusion. Describing this convection is a key step in understanding the interiors of the sun and other stars.

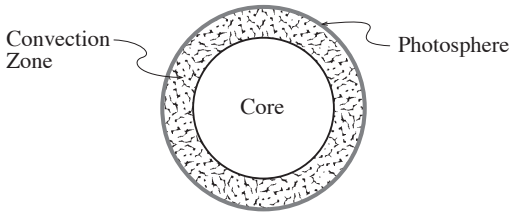

Fig. 16.14: A convection zone occupies the outer 30 per cent of a solar-type star.

A heuristic argument provides the basis for a surprisingly simple description of this convection. As a foundation for our argument, let us identify the relevant physics:

First: the pressure within stars varies through many orders of magnitude; typically 10^{12} for the sun. Therefore, we cannot use the Boussinesq approximation; instead, as a fluid element rises or descends, we must allow for its density to change in response to large changes of the surrounding pressure. Second: The convection involves circulatory motions on such large scales that the attendant shears are small and viscosity is thus unimportant. Third: Because the convection is driven by ineffectiveness of conduction, we can idealize each fluid element as retaining its heat as it moves, so the flow is adiabatic. Fourth: the convection will usually be very subsonic, as subsonic motions are easily sufficient to transport the nuclear-generated heat, except very close to the solar surface.

Our heuristic argument, then, focuses on convecting fluid blobs that move through the star's interior very subsonically, adiabatically, and without viscosity. As the motion is subsonic, each blob will remain in pressure equilibrium with its surroundings. Now, suppose we make a virtual interchange between two blobs at different heights (Fig. 16.15). The blob that rises (blob B in the figure) will experience a decreased pressure and thus will expand, so its density will diminish. If its density after rising is lower than that of its surroundings, then it will be buoyant and continue to rise. Conversely, if the risen blob is denser than its surroundings, then it will sink back to its original location. Therefore, a criterion for convective instability is that the risen blob has lower density than its surroundings. Since the blob and its surroundings have the same pressure, and since the entropy s per unit mass of gas is larger, the lower is its density (there being more phase space available to its particles), the fluid is convectively unstable if the risen blob has a higher entropy than its surroundings. Now, the blob's motion was adiabatic, so its entropy per unit mass s is the same after it rises as before. Therefore, the fluid is convectively unstable if the entropy per unit mass s at the location where the blob began (lower in the star) is greater than that at the location to which it rose (higher in the star); i.e., *the star is convectively unstable if its entropy per unit mass decreases outward,* $ds/dr < 0$. For small blobs, this instability will be counteracted by both viscosity and heat conduction; but for large blobs viscosity and conduction are ineffective, and the convection proceeds.

When building stellar models, astrophysicists find it convenient to determine whether a region of a model is convectively unstable by computing what its structure would be

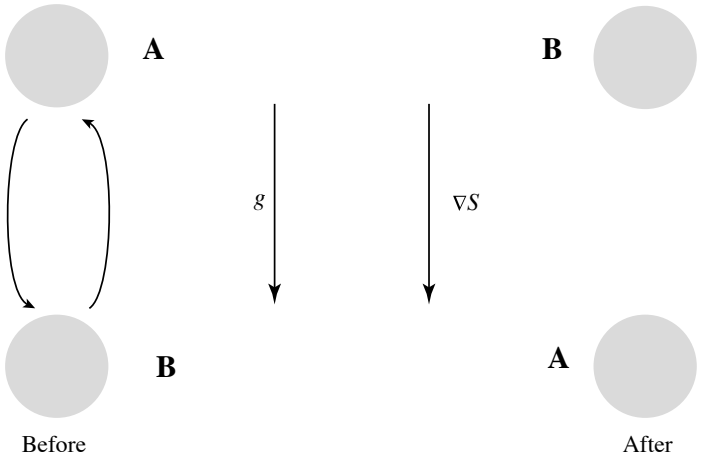

Fig. 16.15: Convectively unstable interchange of two blobs in a star. Blob B rises to the former position of blob A and expands adiabatically to match the surrounding pressure. The entropy per unit mass of the blob is higher than that of the surrounding gas and so the blob has a lower density. It will therefore be buoyant and continue to rise. Similarly, blob A will continue to sink.

without convection, i.e., with all its heat carried radiatively. That computation gives some temperature gradient dT/dr. If this computed dT/dr is *superadiabiatic*, i.e., if

$$-\frac{d\ln T}{d\ln r} > \left(\frac{\partial \ln T}{\partial \ln P}\right)_s \left(-\frac{d\ln P}{d\ln r}\right) \equiv -\left(\frac{d\ln T}{d\ln r}\right)_s \ , \tag{16.119}$$

then correspondingly the entropy s decreases outward, and the star is convectively unstable. This is known as the *Schwarzschild criterion for convection*, since it was formulated by the same Karl Schwarzschild as discovered the Schwarzschild solution to Einstein's equations (which describes a nonrotating black hole; Chap. 25).

In practice, if the star is convective, then the convection is usually so efficient at transporting heat that the actual temperature gradient is only slightly superadiabatic; i.e., the entropy s is nearly independent of radius—it decreases outward only very slightly. (Of course, the entropy can *increase* significantly outwards in a convectively stable zone where radiative diffusion is adequate to transport heat.)

We can demonstrate the efficiency of convection by estimating the convective heat flux when the temperature gradient is slightly superadiabatic, i.e., when $\Delta|\boldsymbol{\nabla} T| \equiv |(dT/dr)| - |(dT/dr)_s|$ is slightly positive. As a tool in our estimate, we introduce the concept of the *mixing length*, denoted by l—the typical distance a blob travels before breaking up. As the blob is in pressure equilibrium, we can estimate its fractional density difference from its surroundings by $\delta\rho/\rho \sim \delta T/T \sim \Delta|\boldsymbol{\nabla} T| l/T$. Invoking Archimedes' principle, we estimate the blob's acceleration to be $\sim g\delta\rho/\rho \sim g\Delta|\boldsymbol{\nabla} T| l/T$ (where g is the local acceleration of gravity), and hence the average speed with which a blob rises or sinks will be $\bar{v} \sim (g\Delta|\boldsymbol{\nabla} T|/T)^{1/2} l$. The convective heat flux is then given by

$$\begin{aligned} F_{\rm conv} &\sim C_P \rho \bar{v} l \Delta|\boldsymbol{\nabla} T| \\ &\sim C_P \rho (g/T)^{1/2} (\Delta|\boldsymbol{\nabla} T|)^{3/2} l^2 \ . \end{aligned} \tag{16.120}$$

We can bring this into a more useful form, accurate to within factors of order unity, by setting the mixing length equal to the pressure scale height $l \sim H = |dr/d\ln P|$ as is usually the case in the outer parts of a star, setting $C_p \sim h/T$ where h is the enthalpy per unit mass [cf. the first law of thermodynamics, Eq. (3) of Box 12.2], setting $g = -(P/\rho)d\ln P/dr \sim c^2|d\ln P/dr|$ [cf. the equation of hydrostatic equilibrium (12.13) and Eq. (16.48d) for the speed of sound c], and setting $|\boldsymbol{\nabla} T| \equiv |dT/dr| \sim T d\ln P/dr$. The resulting expression for $F_{\rm conv}$ can then be inverted to give

$$\frac{|\Delta\boldsymbol{\nabla} T|}{|\boldsymbol{\nabla} T|} \sim \left(\frac{F_{\rm conv}}{h\rho c}\right)^{2/3} \sim \left(\frac{F_{\rm conv}}{\frac{5}{2}P\sqrt{k_B T/m_p}}\right)^{2/3} . \tag{16.121}$$

Here the last expression is obtained from the fact that the gas is fully ionized, so its enthalpy is $h = \frac{5}{2}P/\rho$ and its speed of sound is about the thermal speed of its protons (the most numerous massive particle), $c \sim \sqrt{k_B T/m_p}$ (with k_B Boltzmann's constant and m_p the proton rest mass).

It is informative to apply this estimate to the convection zone of the sun (the outer ~ 30 per cent of its radius; Fig. 16.14). The luminosity of the sun is $\sim 4\times 10^{26}$ W and its radius is 7×10^5 km, so its convective energy flux is $F_{\rm conv} \sim 10^8$ W m^{-2}. Consider, first, the convection zone's base. The pressure there is $P \sim 1$ TPa and the temperature is $T \sim 10^6$ K, so Eq. (16.121) predicts $|\Delta\boldsymbol{\nabla} T|/|\boldsymbol{\nabla} T| \sim 3\times 10^{-6}$; i.e., the temperature gradient at the base of the convection zone need only be superadiabatic by a few parts in a million in order to carry the solar energy flux.

By contrast, at the top of the convection zone (which is nearly at the solar surface), the gas pressure is only ~ 10 kPa and the sound speed is ~ 10 km s^{-1}, so $h\rho c \sim 10^8$W m^{-2}, and $|\Delta\boldsymbol{\nabla} T|/|\boldsymbol{\nabla} T| \sim 1$; i.e., the temperature gradient must depart significantly from the adiabatic gradient in order to carry the heat. Moreover, the convective elements, in their struggle to carry the heat, move with a significant fraction of the sound speed so it is no longer true that they are in pressure equilibrium with their surroundings. A more sophisticated theory of convection is therefore necessary near the solar surface.

Convection is very important in some other types of stars. It is the primary means of heat transport in the cores of stars with high mass and high luminosity, and throughout very young stars before they start to burn their hydrogen in nuclear reactions.

****

EXERCISES

Exercise 16.21 *Problem: Radiative Transport*
The density and temperature in the interior of the sun are roughly 0.1 kg m^{-3} and 1.5×10^7 K.

(a) Estimate the central gas pressure and radiation pressure and their ratio.

(b) The mean free path of the radiation is determined almost equally by Thomson scattering, bound-free absorption and free-free absorption. Estimate numerically the photon

mean free path and hence estimate the photon escape time and the luminosity. How well do your estimates compare with the known values for the sun?

Exercise 16.22 *Problem: Bubbles*
Consider a small bubble of air rising slowly in a large expanse of water. If the bubble is large enough for surface tension to be ignored, then it will form an irregular cap of radius r. Show that the speed with which the bubble rises is roughly $\sim (gr)^{1/2}$. (A more refined estimate gives a numerical coefficient of 2/3.)

****

16.6.5 T2 Double Diffusion — Salt Fingers

Convection, as we have described it so far, is driven by the presence of an unbalanced buoyancy force in an equilibrium distribution of fluid. However, it can also arise as a higher order effect even if the fluid is stably stratified, i.e. if the density gradient is in the same direction as gravity. An example is *salt fingering*, a rapid mixing that can occur when warm, salty water lies at rest above colder fresh water. The higher temperature of the upper fluid initially outbalances the weight of its salt, making it more buoyant than the fresh water below. However, the heat diffuses downward faster than the salt, enabling a density inversion gradually to develop and the salt-rich fluid to begin a slow interchange with the salt-poor fluid below.

It is possible to describe this instability using a local perturbation analysis. The set up is somewhat similar to the one we used in Sec. 16.6.3 to analyze Rayleigh-Bénard convection: We consider a stratified fluid in which there is a vertical gradient in the temperature, and as before, we measure its departure from a reference temperature T_0 at a midplane ($z = 0$) by $\tau \equiv T - T_0$. We presume that in the equilibrium τ varies linearly with z, so $\boldsymbol{\nabla}\tau = (d\tau/dz)\mathbf{e}_z$ is constant. Similarly, we characterize the salt concentration by $C \equiv$ (concentration) − (equilibrium concentration at the mid plane), and we assume that in equilibrium C like τ varies linearly with height, so $\boldsymbol{\nabla}C = (dC/dz)\mathbf{e}_z$ is constant. The density ρ will be equal to the equilibrium density at the midplane plus corrections due to thermal expansion and due to salt concentration

$$\rho = \rho_0 - \alpha\rho_0\tau + \beta\rho_0 C \tag{16.122}$$

[cf. Eq. (16.97)]. Here β is a constant for concentration analogous to the thermal expansion coefficient α for temperature. In this problem, by contrast with Rayleigh-Bénard convection, it is easier to work directly with the pressure than the modified pressure. In equilibrium, hydrostatic equilibrium dictates that its gradient be $\boldsymbol{\nabla}P = -\rho\boldsymbol{g}$.

Now, let us perturb about these values and write down the linearized equations for the evolution of the perturbations. We shall denote the perturbation of temperature (relative to the reference temperature) by $\delta\tau$, of salt concentration by δC, of density by $\delta\rho$, of pressure by δP, and of velocity by simply $\mathbf{v}$ since the unperturbed state has $\mathbf{v} = 0$. We shall not ask about the onset of instability, but rather (because we expect our situation to be generically unstable) we shall seek a dispersion relation $\omega(\mathbf{k})$ for the perturbations. Correspondingly,

in all our perturbation equations we shall replace $\partial/\partial t$ with $-i\omega$ and $\boldsymbol{\nabla}$ with $i\mathbf{k}$, except for the equilibrium $\boldsymbol{\nabla}C$ and $\boldsymbol{\nabla}\tau$ which are constants.

The first of our perturbation equations is the linearized Navier-Stokes equation

$$-i\omega\rho_0\mathbf{v} = -i\mathbf{k}\delta P + \boldsymbol{g}\delta\rho - \nu k^2\rho_0\mathbf{v} \ , \tag{16.123}$$

where we have kept the viscous term because we expect the Prandtl number to be of order unity (for water Pr ~ 6). Low velocity implies incompressibity $\boldsymbol{\nabla}\cdot\mathbf{v} = 0$, which becomes

$$\mathbf{k}\cdot\mathbf{v} = 0 \ . \tag{16.124}$$

The density perturbation follows from the perturbed form of Eq. (16.122)

$$\delta\rho = -\alpha\rho_0\delta\tau + \beta\rho_0\delta C \ . \tag{16.125}$$

The temperature perturbation is governed by Eq. (16.103) which linearizes to

$$-i\omega\delta\tau + (\mathbf{v}\cdot\boldsymbol{\nabla})\tau = -\chi k^2\delta\tau \ . \tag{16.126}$$

Assuming that the timescale for the salt to diffuse is much longer than the temperature to diffuse, we can ignore salt diffusion all together so that $d\delta C/dt = 0$, which becomes

$$-i\omega\delta C + (\mathbf{v}\cdot\boldsymbol{\nabla})C = 0 \tag{16.127}$$

Equations (16.123)–(16.127) are five equations for the five unknowns $\delta P, \delta\rho, \delta C, \delta T, \mathbf{v}$, one of which is a three component vector! Unless we are careful, we will end up with a seventh order algebraic equation. Fortunately, there is a way to keep the algebra manageable. First, we eliminate the pressure perturbation by taking the curl of Eq. (16.123) [or equivalently by crossing $\mathbf{k}$ into Eq. (16.123)]:

$$(-i\omega + \nu k^2)\rho_0\mathbf{k}\times\mathbf{v} = \mathbf{k}\times\boldsymbol{g}\delta\rho \tag{16.128}$$

Taking the curl of this equation again allows us to incorporate incompressibility (16.124):

$$(i\omega - \nu k^2)\rho_0 k^2\boldsymbol{g}\cdot\mathbf{v} = [(\mathbf{k}\cdot\boldsymbol{g})^2 - k^2g^2]\delta\rho \ . \tag{16.129}$$

Since $\boldsymbol{g}$ points vertically, this is one equation for the density perturbation in terms of the vertical velocity perturbation v_z . We can obtain a second equation of this sort by inserting Eq. (16.126) for $\delta\tau$ and Eq. (16.127) for δC into Eq. (16.125); the result is

$$\delta\rho = -\left(\frac{\alpha\rho_0}{i\omega - \chi k^2}\right)(\mathbf{v}\cdot\boldsymbol{\nabla})\tau + \frac{\beta\rho_0}{i\omega}(\mathbf{v}\cdot\boldsymbol{\nabla})C \ . \tag{16.130}$$

Since the unperturbed gradients of temperature and salt concentration are both vertical, Eq. (16.130), like (16.129), involves only v_z and not v_x or v_y. Solving both (16.129) and (16.130) for the ratio $\delta\rho/v_z$ and equating these two expressions, we obtain the following dispersion relation for our perturbations:

$$\omega(\omega + i\nu k^2)(\omega + i\chi k^2) + \left[1 - \frac{(\mathbf{k}\cdot\boldsymbol{g})^2}{k^2g^2}\right][\omega\alpha(\boldsymbol{g}\cdot\nabla)\tau - (\omega + i\chi k^2)\beta(\boldsymbol{g}\cdot\nabla)C] = 0 \ . \tag{16.131}$$

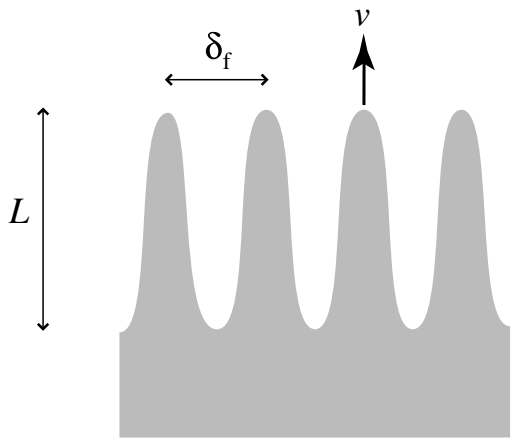

Fig. 16.16: Salt Fingers in a fluid in which warm, salty water lies on top of cold fresh water.

When $\mathbf{k}$ is real, as we shall assume, we can write this dispersion relation as a cubic equation for $p = -i\omega$ with real coefficients. The roots for p are either all real or one real and two complex conjugates, and growing modes have the real part of p positive. When the constant term in the cubic is negative, i.e. when

$$(\boldsymbol{g} \cdot \nabla)C < 0 \,, \tag{16.132}$$

we are guaranteed that there will be at least one positive, real root p and this root will correspond to an unstable, growing mode. Therefore, a sufficient condition for instability is that the concentration of salt increase with height!

By inspecting the dispersion relation we conclude that the growth rate will be maximal when $\mathbf{k}\cdot\boldsymbol{g} = 0$, i.e. when the wave vector is horizontal. What is the direction of the velocity $\mathbf{v}$ for these fastest growing modes? Incompressibility (16.124) says that $\mathbf{v}$ is orthogonal to the horizontal $\mathbf{k}$; and Eq. (16.128) says that $\mathbf{k} \times \mathbf{v}$ points in the same direction as $\mathbf{k} \times \boldsymbol{g}$, which is horizontal since $\boldsymbol{g}$ is vertical. These two conditions imply that $\mathbf{v}$ points vertically. Thus, these fastest modes represent *fingers* of salty water descending past rising fingers of fresh water; cf. Fig. 16.16. For large k (narrow fingers), the dispersion relation (16.131) predicts a growth rate given approximately by

$$i\omega \sim \frac{\beta(\boldsymbol{g} \cdot \nabla)C}{\nu k^2} \,. \tag{16.133}$$

Thus, the growth of narrow fingers is driven by the concentration gradient and retarded by viscosity. For larger fingers, the temperature gradient will participate in the retardation, since the heat must diffuse in order to break the buoyant stability.

Now let us turn to the nonlinear development of this instability. Although we have just considered a single Fourier mode, the fingers that grow are roughly cylindrical rather than sheet-like. They lengthen at a rate that is slow enough for the heat to diffuse horizontally, though not so slow that the salt can diffuse. Let the diffusion coefficient for the salt be χ_C by analogy with χ for temperature. If the length of the fingers is L and their width is δ_f,

then to facilitate heat diffusion and prevent salt diffusion, the vertical speed v must satisfy

$$\frac{\chi_C\, L}{\delta_f^2} \ll v \ll \frac{\chi\, L}{\delta_f^2}\ . \tag{16.134}$$

Balancing the viscous acceleration $v\nu/\delta_f^2$ by the buoyancy acceleration $g\beta\delta C$, we obtain

$$v \sim \frac{g\beta\delta C\delta_f^2}{\nu}\ . \tag{16.135}$$

We can therefore re-write Eq. (16.134) as

$$\left(\frac{\chi_C\nu L}{g\beta\delta C}\right)^{1/4} \ll \delta_f \ll \left(\frac{\chi\nu L}{g\beta\delta C}\right)^{1/4}\ . \tag{16.136}$$

Typically, $\chi_C \sim 0.01\chi$, so Eq. (16.136) implies that the widths of the fingers lie in a narrow range, as is verified in laboratory experiments.

Salt fingering can also occur naturally, for example in an estuary where cold river water flows beneath sea water warmed by the sun. However, the development of salt fingers is quite slow and in practice it only leads to mixing when the equilibrium velocity field is very small. This instability is one example of a quite general type of instability known as *double diffusion* which can arise when two physical quantities can diffuse through a fluid at different rates. Other examples include the diffusion of two different solutes and the diffusion of vorticity and heat in a rotating flow.

****

EXERCISES

Exercise 16.23 *Problem: Laboratory experiment*
Make an order of magnitude estimate of the size of the fingers and the time it takes for them to grow in a small transparent jar. You might like to try an experiment.

Exercise 16.24 *Problem: Internal Waves*
Consider a stably stratified fluid at rest and let there be a small (negative) vertical density gradient, $d\rho/dz$.

(a) By modifying the above analysis, ignoring the effects of viscosity, heat conduction and concentration gradients, show that small-amplitude linear waves, which propagate in a direction making an angle θ to the vertical, have an angular frequency given by $\omega = N|\sin\theta|$, where $N \equiv [(\mathbf{g}\cdot\nabla)\ln\rho]^{1/2}$ is known as the *Brunt-Väisälä frequency*. These waves are called *internal waves*.

(b) Show that the group velocity of these waves is orthogonal to the phase velocity and interpret this result physically.

****

Box 16.4
Important Concepts in Chapter 15

- Gravity waves on water and other liquids, Sec. 16.2
  - Deep water waves and shallow water waves, Secs. 16.2.1, 16.2.2
  - Tsunamis, Ex. 16.6
  - Dispersion, Sec. 16.3.1
  - Steepening due to nonlinear effects, Sec. 16.3.1, Fig. 16.4
  - Solitons or solitary waves; nonlinear steepening balances dispersion, Sec. 16.3
  - Korteweg-deVries equation, Secs. 16.3.1–16.3.4
- Surface tension and its stress tensor, Box 16.2
  - Capillary waves, Sec. 16.2.3
- Rossby Waves in a Rotating Fluid, Sec. 16.4
- Sound waves in fluids and gases, Sec. 16.5
  - Sound wave generation in slow-motion approximation: power proportional to squared time derivative of monopole moment, Sec. 16.5.2
  - Decibel, Sec. 16.5.2
  - Matched asymptotic expansions, Sec. 16.5.3
  - Radiation reaction force; runaway solution as a spurious solution that violates the slow-motion approximation used to derive it, Sec. 16.5.3
- Thermal effects and convection, Sec. 16.6
  - Coefficient of thermal conductivity, κ, and diffusive heat conduction, Sec. 16.6.1
  - Thermal diffusivity, $\chi = \kappa/\rho C_p$, and diffusion equation for temperature, Sec. 16.6.1
  - Thermal expansion coefficient, $\alpha = (\partial \ln \rho/\partial T)_P$, Sec. 16.6.2
  - Prandtl number, Pr= ν/χ $\sim$(vorticity diffusion)/(heat diffusion), Sec. 16.6.1
  - Péclet number, Pe= VL/χ $\sim$(advection)/(conduction), Sec. 16.6.1
  - Rayleigh number Ra=$\alpha g/\Delta T d^3/(\nu\chi)$ $\sim$(buoyancy)/(viscous force), Sec. 16.6.3
  - Boussinesq approximation for analyzing thermally induced buoyancy, Sec. 16.6.2
  - Free convection and forced convection, Sec. **??**
  - Rayleigh-Bénard (free) convection, Sec. 16.6.3 and Fig. 16.11
  - Critical Rayleigh number for onset of Rayleigh-Bénard convection, Sec. 16.6.3
  - Schwarzschild criterion for convection in stars, Sec. 16.6.4
  - Double-diffusion instability, Sec. 16.6.5

Bibliographic Note

For textbook treatments of waves in fluids, we recommend Lighthill (1978) and Whitham (1974), and from a more elementary and physical viewpoint, Tritton (1977). To develop physical insight into gravity waves on water and sound waves in a fluid, we suggest portions of the movie by Bryson (1964). For solitary-wave solutions to the Korteweg-deVries equation, see materials, including brief movies, at the website of Takasaki (2006).

For a brief, physically oriented introduction to Rayleigh-Bénard convection see Chap. 4 of Tritton (1987). In their Chaps. 5 and 6, Landau and Lifshitz (1959) give a fairly succinct treatment of diffusive heat flow in fluids, the onset of convection in several different physical situations, and the concepts underlying double diffusion. In his Chaps. 2–6, Chandrasekhar (1961) gives a thorough and rich treatment of the influence of a wide variety of phenomena on the onset of convection, and on the types of fluid motions that can occur near the onset of convection. The book by Turner (1973) is a thorough treatise on the influence of buoyancy (thermally induced and otherwise) on fluid motions. It includes all topics treated in Sec. 16.6 and much much more.

Bibliography

Bryson, A.E. 1964. *Waves in Fluids*, a movie (National Committee for Fluid Mechanics Films); available at `http://web.mit.edu/hml/ncfmf.html` .

Burke, W. W. 1970. "Runaway solutions: remarks on the asymptotic theory of radiation damping," *Phys. Rev. A* **2**, 1501–1505.

Chandrasekhar, S. 1961. *Hydrodynamics and Hydromagnetic Stability* Oxford:Oxford University Press00

Cole, J. 1974. *Perturbation Methods in Applied Mathematics*, Waltham Mass: Blaisdell.

Chelton, D.B. and Schlax, M.G. (1996). "Global observations of oceanic Rossby waves", *Science*, **272**, 234.

Fultz, D. 1969. *Rotating Flows*, a movie (National Committee for Fluid Mechanics Films); available at `http://web.mit.edu/hml/ncfmf.html` .

Gill, A. E. 1982. *Atmosphere Ocean Dynamics*, New York: Academic Press.

Greenspan, H. P. 1973. *The Theory of Rotating Fluids*, Cambridge: Cambridge University Press.

Jackson, J. D. 1999. *Classical Electrodynamics*, third edition, New York: Wiley.

Landau, L. D. and Lifshitz, E. M. 1959. *Fluid Dynamics*, Oxford: Pergamon.

Libbrecht, K. G. & Woodard, M. F. 1991. *Science*, **253**, 152.

Lighthill, M. J. 1978. *Waves in Fluids*, Cambridge: Cambridge University Press.

Pellew, A. and Southwell, R. V. 1940. *Proceedings of the Royal Society*, **A176**, 312.

Rorlich, F. 1965. *Classical Charged Particles*, Reading Mass: Addison Wesley.

Scott-Russell, J. 1844. *Proc. Roy. Soc. Edinburgh*, 319 (1844).

Takasaki, K. 2006. *Many Faces of Solitons*,
http://www.math.h.kyoto-u.ac.jp/ takasaki/soliton-lab/gallery/solitons/kdv-e.html .

Tritton, D. J. 1987. *Physical Fluid Dynamics*, Oxford: Oxford Science Publications.

Turcotte, D. L. and Schubert, G. 1982. *Geodynamics*, New York: Wiley.

Turner, J. S. 1973. *Buoyancy Effects in Fluids*, Cambridge: Cambridge University Press.

Whitham, G. B. 1974. *Linear and Non-Linear Waves*, New York: Wiley.